LA-UR-19-21428

Approved for public release; distribution is unlimited.

Title: Implicit, manifold-preserving numerical representations and solvers for multiscale kinetic simulations of plasmas

Author(s): Chacon, Luis
Chen, Guangye
Taitano, William
Simakov, Andrei N.
Barnes, Daniel C.

Intended for: Web

Issued: 2019-02-21

Los Alamos
NATIONAL LABORATORY
EST. 1943

National Nuclear Security Administration
Operated by TRIAD National Security for the U.S. Department of Energy's NNSA

Implicit, manifold-preserving numerical representations and solvers for multiscale kinetic simulations of plasmas

Courant Institute Colloquium, NYU

Feb. 11th, 2019

Luis Chacón

In collaboration (over the years) with:

G. Chen

D. C. Barnes

W. Taitano

A. Simakov

Operated by TRIAD National Security, LLC for the U.S. Department of Energy's NNSA

Agenda

Feb. 11th, 2019

Courant Institute Colloquium

- Manifold-preserving algorithms for multiscale kinetic simulations
- Collisionless plasmas: conservative, implicit particle-in-cell algorithms
- Collisional plasmas: conservative, implicit, adaptive Vlasov-Fokker-Planck algorithms for ICF applications

Los Alamos NATIONAL LABORATORY EST. 1943

Manifold-preserving algorithms for multiscale kinetic simulations

- **High-fidelity simulation of kinetic multiscale problems require solving the kinetic transport equation, e.g.:**
  - Boltzmann (rarefied gas dynamics, radiation transport)
  - Vlasov-Fokker-Planck (collisional plasmas)
- **Numerical challenges of kinetic descriptions are many:**
  - High dimensional (3D+3V+time), highly nonlinear, exceeding multiscale
  - Cannot afford to run fully resolved in time or space, even with most powerful supercomputers
  - Need to constrain numerical errors as much as possible
- **Manifold-preserving discrete algorithms control numerical error by preserving *constraints and asymptotic properties* of the continuum problem, e.g., conservation laws. They facilitate:**
  - Asymptotic well-posedness
  - *Discrete* model nesting (e.g., Boltzmann → Navier-Stokes → Euler)
  - Avoiding long-term manifold drift [O(1) errors!]
- **Implicit timestepping is needed for efficiency.**
  - Model-nesting can be effectively used for algorithmic acceleration (e.g., moment-based acceleration, aka High-Order/Low-Order, micro-macro, etc).
- **We have applied these ideas to rarefied gases, radiation, and plasmas.**
- **We will focus on plasmas throughout this talk.**

First-principles simulation of plasmas: The Vlasov-Fokker-Planck-Maxwell system

➤**A fully ionized plasma**: soup of ions, electrons, coupled by EM fields

➤Probability distribution function f_s described by Vlasov-Fokker-Planck eq.

$$\partial_t f_s + \mathbf{v} \cdot \nabla f_s + \frac{q}{m}(\mathbf{E} + \mathbf{v} \times \mathbf{B}) \cdot \nabla_v f_s = \boxed{\left(\frac{\partial f}{\partial t}\right)_c} \longrightarrow \text{Fokker-Planck-Landau}$$

coupled with Maxwell equations (or Darwin, ES, etc):

$$\begin{aligned} \partial_t \mathbf{B} + \nabla \times \mathbf{E} &= 0 \\ -\mu_0 \epsilon_0 \partial_t \mathbf{E} + \nabla \times \mathbf{B} &= \mu_0 \boxed{\mathbf{j}} \\ \nabla \cdot \mathbf{B} &= 0 \\ \nabla \cdot \mathbf{E} &= \frac{\boxed{\rho}}{\epsilon_0} \end{aligned}$$

$$\longrightarrow \mathbf{j} = \sum_s \int q \mathbf{v} f_s d\mathbf{v} \ ; \ \rho = \sum_s \int q f_s d\mathbf{v}$$

➤**Manifold constraints**: positivity of f_s, strict conservation of charge (mass), momentum, and energy, H-theorem

➤**Very rich manifold asymptotics**: quasineutrality, ambipolarity, multi-fluid, resistive MHD, ideal MHD

Challenges of first-principles kinetic plasma simulations

➤**High dimensionality (3D+3V+time), nonlinear, exceedingly multiscale**

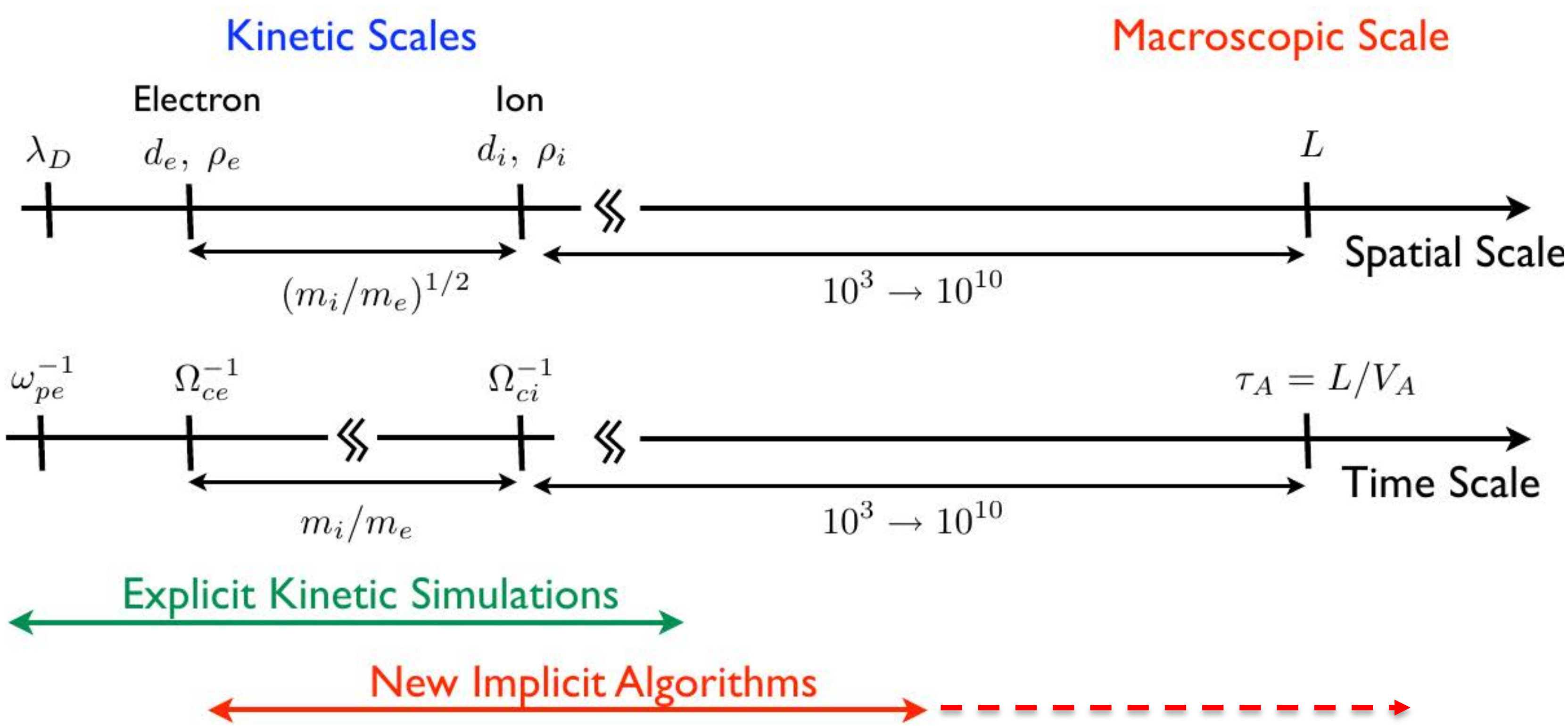

➤**Goal: integrate electron-ion-field kinetic system on engineering time and length scales while capturing kinetic effects.**

- Need asymptotic-preserving implicit methods, adaptivity in phase space, strict conservation properties

Manifold-preserving implicit Lagrangian (PIC) methods for collisionless plasmas

Vlasov-Maxwell equation for collisionless plasmas

- **Vlasov equation**

$$\partial_t f_s + \mathbf{v}\cdot\nabla f_s + \frac{q_s}{m_s}(\mathbf{E}+\mathbf{v}\times\mathbf{B})\cdot\nabla f_s = \boxed{0}$$

coupled with Maxwell equations

$$\begin{aligned}
\partial_t \mathbf{B} + \nabla\times\mathbf{E} &= 0 \\
-\mu_0\epsilon_0\partial_t\mathbf{E} + \nabla\times\mathbf{B} &= \mu_0\mathbf{j} \\
\nabla\cdot\mathbf{B} &= 0 \\
\nabla\cdot\mathbf{E} &= \frac{\rho}{\epsilon_0}
\end{aligned}$$

where:

$$\mathbf{j} = \sum_s \int q\mathbf{v} f_s d\mathbf{v} \;\; ; \;\; \rho = \sum_s \int q f d\mathbf{v}$$

- **Vlasov equation is a singular limit of VFP**
  - Features an infinite number of invariants (any function of f_s)
  - However, only mass, momentum, and energy survive with arbitrarily infrequent collisions

Lagrangian (particle-in-cell, PIC) discretization of the Vlasov-Maxwell system

- Lagrangian solution by the **method of characteristics**:

$$f(\mathbf{x},\mathbf{v},t) = f_0\left(\mathbf{x} - \int_0^t dt\mathbf{v}, \mathbf{v} - \frac{1}{m}\int_0^t dt\mathbf{F}\right) \; ; \; \mathbf{x}(t=0) = \mathbf{x}_0 \; ; \; \mathbf{v}(t=0) = \mathbf{v}_0$$

- PIC approach follows characteristics employing **macroparticles** (volumes in phase space)
- Maxwell's equations are usually solved by finite-difference time-domain methods.

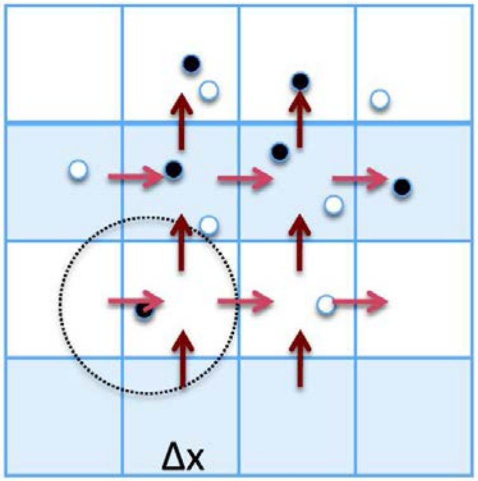

$$f(\mathbf{x},\mathbf{v},t) = \sum_p \delta(\mathbf{x}-\mathbf{x}_p)\delta(\mathbf{v}-\mathbf{v}_p)$$

$$\begin{aligned} \dot{\mathbf{x}}_p &= \mathbf{v}_p \\ \dot{\mathbf{v}}_p &= \frac{q_p}{m_p}(\mathbf{E} + \mathbf{v}\times\mathbf{B}) \end{aligned}$$

FDTD

$$\begin{aligned} \partial_t\mathbf{B} + \nabla\times\mathbf{E} &= 0 \\ -\mu_0\epsilon_0\partial_t\mathbf{E} + \nabla\times\mathbf{B} &= \mu_0\mathbf{j} \\ \nabla\cdot\mathbf{B} &= 0 \\ \nabla\cdot\mathbf{E} &= \frac{\rho}{\epsilon_0} \end{aligned}$$

$$\boxed{\delta(\mathbf{x}-\mathbf{x}_p) \longrightarrow S(\mathbf{x}-\mathbf{x}_p) \; ; \; E_p = \sum_i E_i S(x_i - x_p) \; ; \; j_i = \sum_p j_p S(x_i - x_p)}$$

Classical PIC algorithm is explicit (i.e., not multiscale, not conservative)

- Classical explicit PIC: "leap-frogs" particle positions and velocities, field-solve at position update:

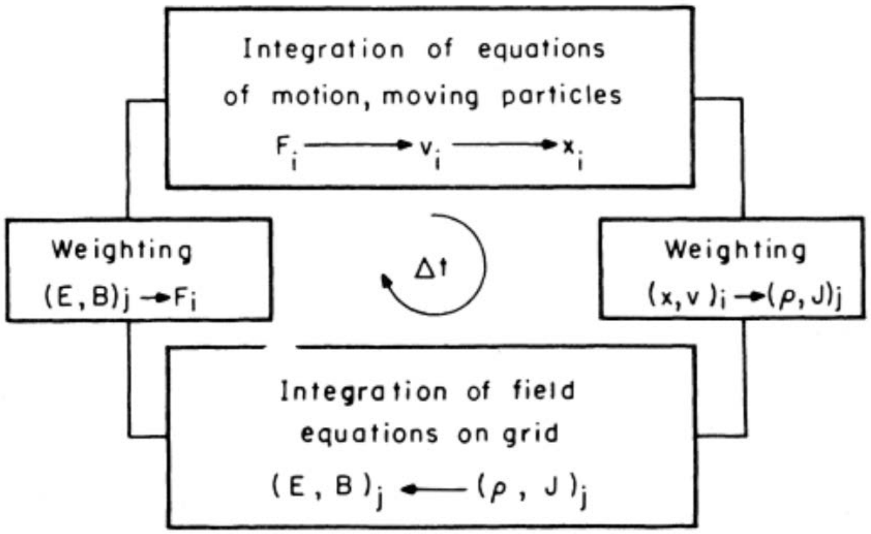

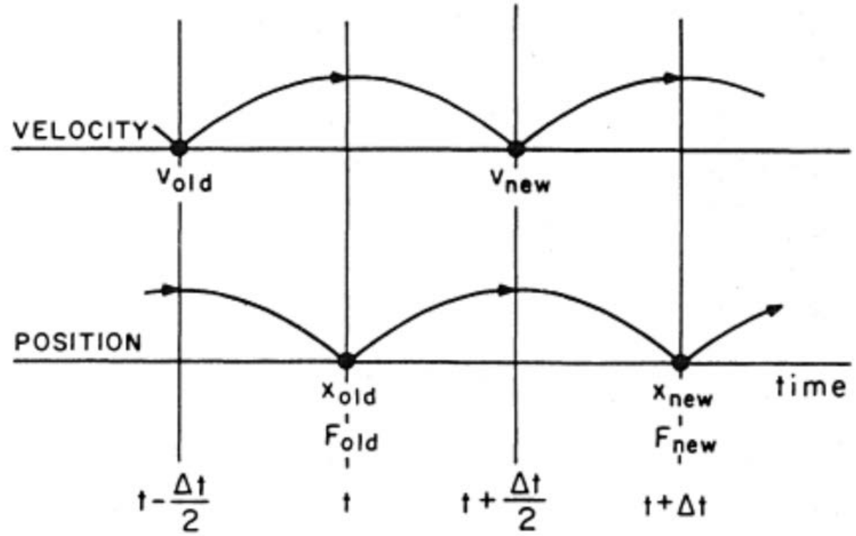

- Implementation is straightforward, but...
- Performance limitations:
  - CFL-type instability: $\min(\omega_{pe}\Delta t < 1,\, c\Delta t < \Delta x)$. **Minimum temporal resolution**
  - Finite-grid instability: $\Delta x < \lambda_{Debye}$. **Minimum spatial resolution**
  - Memory bounded: challenging for efficient use of modern computer architectures.
- Accuracy limitations:
  - **Lack of energy conservation**, problematic for long-time-scale simulations
- To remove the stability/accuracy constraints of explicit methods, we consider implicit methods.

What about implicit PIC?

- **Exploration of implicit PIC started in the 1980s**
  - Implicit moment method[1]
  - Direct implicit method[2]
- **Early approaches used linearized, semi-implicit formulations:**
  - Lack of nonlinear convergence
  - Particle orbit accuracy (particle and fields integrated in lock-step)
  - Inconsistencies between particles and moments
  - Inaccuracies! → Plasma self-heating/cooling[3]
- **Our approach: nonlinear implicit PIC**
  - Enforcing nonlinear convergence; consistency between particles, moments, and fields.
  - Ensuring exact global energy conservation and local charge conservation properties.
  - Allowing adaptivity in both time and space without loss of the conservation properties.
  - Allowing **moment-based preconditioning** to *accelerate* the *iterative* kinetic solver!

1. Mason, R. J. (1981), Brackbill, J. U., and Forslund, D. W. (1982)
2. Friedman, A., Langdon, A. B. and Cohen, B. I.(1981)
3. Cohen, B. I., Langdon, A. B., Hewett, D. W., and Procassini, R. J. (1989)

Fully implicit PIC: 1D electrostatic PIC

Chen et al, JCP 2011, 2012, 2013; Taitano et al, SISC (2013)

Fully implicit 1D electrostatic PIC formulation

- A fully implicit formulation couples particles and fields non-trivially (integro-differential PDE):

$$\frac{f^{n+1}-f^n}{\Delta t}+\mathbf{v}\cdot\nabla\frac{f^{n+1}+f^n}{2} \quad - \quad \frac{q}{m}\nabla\frac{\Phi^{n+1}+\Phi^n}{2}\cdot\nabla_{\mathbf{v}}\frac{f^{n+1}+f^n}{2}=0$$

$$\nabla^2\Phi^{n+1} \quad = \quad \int d\mathbf{v}\, f^{n+1}(\mathbf{x},\mathbf{v},t)$$

- In PIC, f^{n+1} is sampled by a large collection of particles in phase space, $\{\mathbf{x},\mathbf{v}\}_p^{n+1}$.
  - There are N_p particles, each particle requiring $2\times d$ equations ($d \rightarrow$dimensions),
  - Field requires N_g equations, one per grid point.
- If implemented naively, an impractically large algebraic system of equations results:

$$\boxed{\mathbf{F}(\{\mathbf{x},\mathbf{v}\}_p^{n+1},\{\Phi^{n+1}\}_g)=0} \rightarrow \dim(\mathbf{F})=2dN_p+N_g$$

  - No current computing mainframe can afford the memory requirements
  - Algorithmic issues are showstoppers (e.g., how to precondition it?)
- An alternative strategy exists: nonlinear elimination (**particle enslavement**)

Particle enslavement (nonlinear elimination)

- Full residual $\mathbf{F}(\{x, v\}_p, \{\Phi\}_g) = 0$ is impractical to implement
- Alternative: nonlinearly eliminate particle quantities **so that they are not dependent variables**:
  - Formally, particle equations of motion are functionals of the electrostatic potential:

$$x_p^{n+1} = x_p[\Phi^{n+1}] \; ; \; v_p^{n+1} = v_p[\Phi^{n+1}]$$

$$\mathbf{F}(\mathbf{x}_p{}^{n+1}, \mathbf{v}_p{}^{n+1}, \mathbf{\Phi}^{n+1}) = \mathbf{F}(\mathbf{x}[\mathbf{\Phi}^{n+1}], \mathbf{v}[\mathbf{\Phi}^{n+1}], \mathbf{\Phi}^{n+1}) = \tilde{\mathbf{F}}(\mathbf{\Phi}^{n+1})$$

Nonlinear residual can be *unambiguously* formulated in terms of electrostatic potential only!

- Nonlinear solver storage requirements are dramatically decreased, making it tractable:
  - Nonlinear solver storage requirements $\propto N_g$, **comparable to a fluid simulation**
  - Particle quantities $\Rightarrow$ auxiliary variables: only a **single copy of particle population** needs to be maintained in memory throughout the nonlinear iteration

Nonlinear solver: Jacobian-free Newton-Krylov

- After spatial and temporal discretization $\Rightarrow$ a large set of nonlinear equations: $\boxed{\boldsymbol{F}(\boldsymbol{x}^{n+1}) = \boldsymbol{0}}$
- Converging nonlinear couplings requires iteration
- We begin with Newton's linearization:

$$\boxed{\boldsymbol{x}^{k+1} = \boldsymbol{x}^k - J_k^{-1}\boldsymbol{F}(\boldsymbol{x}^k)}$$

- Jacobian matrix inversion requires a linear solver $\Rightarrow$ Krylov subspace methods (GMRES)
  - Only require matrix-vector products to proceed.
  - Jacobian-vector product can be computed Jacobian-free (**CRITICAL**: no need to form Jacobian matrix):

$$\left(\frac{\partial \boldsymbol{F}}{\partial \boldsymbol{x}}\right)_k \boldsymbol{y} = J_k \boldsymbol{y} = \lim_{\epsilon \to 0} \frac{\boldsymbol{F}(\boldsymbol{x}^k + \epsilon \boldsymbol{y}) - \boldsymbol{F}(\boldsymbol{x}^k)}{\epsilon}$$

  - Krylov methods can be easily preconditioned: $P_k^{-1} \sim J_k^{-1}$

$$J_k P_k^{-1} P_k \delta \boldsymbol{x} = -\boldsymbol{F}_k$$

We will explore moment-based preconditioning strategies later in this talk.

An important detail: Vlasov-Poisson vs. Vlasov-Ampere

- Two *equivalent* formulations are possible:

1D Vlasov-Poisson (VP)	1D Vlasov-Ampère (VA)
$\partial_t f + v\partial_x f + \frac{qE}{m}\partial_v f = 0$ $\partial_x E = \frac{\rho}{\epsilon_0}$ $E = -\partial_x \Phi$	$\partial_t f + v\partial_x f + \frac{qE}{m}\partial_v f = 0$ $\epsilon_0 \partial_t E + j = \langle j \rangle$
Two systems are equivalent in continuum, but not in the discrete.	
• Conventionally used in explicit PIC. • Exact *local* charge conservation. • Exact *global* momentum conservation. • Unstable with orbit averaging in implicit context [Cohen and Freis, 1982].	• Exact *local* charge conservation. • Exact *global* energy conservation. • Suitable for orbit averaging. • Can be extended to electromagnetic system in multi-D.

- We consider Vlasov-Ampere to derive discrete conservative formulation.

Details of enslaved nonlinear residual evaluation

- The nonlinear residual formulation $\mathbf{F}(E^{n+1})$ based on Vlasov-Ampere formulation is as follows:
  1. Input E (given by JFNK iterative method)
  2. Move particles (i.e., find $x_p[E]$, $v_p[E]$ by solving equations of motion)
     (a) Requires inner (local) nonlinear iteration: Picard (not stiff)
     (b) Can be as complicated as we desire (substepping, adaptivity, etc)
  3. Compute moments (current)
  4. Form Vlasov-Ampere equation residual
  5. return
- Full implicitness **enables exact global energy conservation**! (CRITICAL)
- Because particle move is performed within function evaluation, we have much freedom.
- We can explore improvements in particle mover to ensure **long-term accuracy!**
  - **Multi-rate integrators** (ensures orbit accuracy)
  - **Exact charge conservation strategy** (a new charge-conserving particle mover)

Fully implicit discretization: Exact energy conservation

- Fully implicit Crank-Nicolson time discretization:

$$\varepsilon_0 \frac{E_i^{n+1} - E_i^n}{\Delta t} + j_i^{n+1/2} - \langle j \rangle = 0;$$

$$\frac{x_p^{n+1} - x_p^n}{\Delta t} - v_p^{n+1/2} = 0;$$

$$\frac{v_p^{n+1} - v_p^n}{\Delta t} - \frac{q_p}{m_p} \sum_i E_i^{n+1/2} S(x_i - x_p^{n+1/2}) = 0;$$

$$j_i^{n+1/2} = \sum_p q_p v_p^{n+1/2} S(x_p^{n+1/2} - x_i).$$

- C-N enforces energy conservation to numerical round-off:

$$\sum_p \frac{m_p}{2}(v_p^{n+1} + v_p^n)(v_p^{n+1} - v_p^n) = -\sum_i \varepsilon_0 \frac{E_i^{n+1} - E_i^n}{\Delta t} \frac{E_i^{n+1} + E_i^n}{2} \Rightarrow \boxed{\sum_p \frac{1}{2} m_p v_p^2 + \sum_i \frac{1}{2} \varepsilon_0 E_i^2 = \text{const}}$$

  - No CFL condition.
  - Robust against finite-grid instabilities
  - Requires that particles and fields are nonlinearly converged.

Multirate particle integrator: Exact charge conservation

- Multi-rate particle integrator: field time-scale $\Delta t \gg$ orbit time-scale $\Delta\tau$

  Accurate orbit integration requires particle sub-stepping!

- Local charge conservation $\partial_t \rho + \nabla \cdot \mathbf{j} = 0$ is essential to ensure long-term accuracy.
  - Derived independently from *both* Vlasov and Maxwell equations: "glues" them together.
- B-spline interpolation ensures charge conservation within cell boundaries; broken when particles cross cell boundaries.
  - **Standard strategy** based on current redistribution when particle crosses boundary.[4]
  - Current redistribution breaks energy conservation. **Need a new strategy**.
- Particles stop at cell boundaries $\Rightarrow$ exact charge conservation for B-splines with order$\leq$2

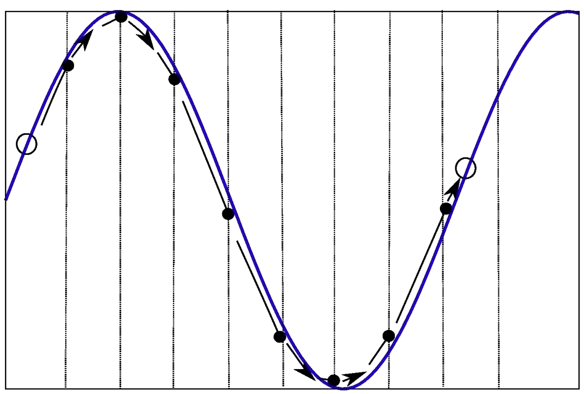

$$\left.\begin{aligned} \rho_{i+\frac{1}{2}} &= \textstyle\sum_p q_p \frac{S_m(x-x_{i+\frac{1}{2}})}{\Delta x} \\ j_i &= \textstyle\sum_p q_p v_p \frac{S_{m-1}(x-x_i)}{\Delta x} \\ S'_m(x) &= \frac{S_{m-1}(x+\frac{\Delta x}{2}) - S_{m-1}(x-\frac{\Delta x}{2})}{\Delta x} \end{aligned}\right\} \overset{(m=1,2)}{\Longrightarrow} [\partial_t \rho + \nabla \cdot \mathbf{j} = 0]_{i+\frac{1}{2}}^{n+\frac{1}{2}} = 0$$

[4] Buneman 1968, Morse and Nielson, 1971

Multirate particle integrator: Recover energy conservation

- Particle substepping breaks energy conservation.
- Energy conservation theorem can be recovered by orbit averaging Ampère's law:

$$\epsilon_0 \partial_t E + j = \langle j \rangle \quad , \quad \frac{1}{\Delta t}\int_t^{t+\Delta t} d\tau [\cdots] \Rightarrow \boxed{\epsilon_0 \frac{E^{n+1} - E^n}{\Delta t} + \bar{j} = \langle \bar{j} \rangle}$$

- Orbit-averaged current is found as: [Cohen and Freis, 1982]

$$\bar{j} = \frac{1}{\Delta t}\int_t^{t+\Delta t} d\tau \, j \approx \frac{1}{\Delta t}\sum_p \sum_{\nu=1}^{N_\nu} q_p v_p S(x - x_p)\Delta\tau^\nu$$

- With these definitions, exact energy conservation is recovered:

$$\sum_p \sum_\nu \frac{m_p}{2}(v_p^{\nu+1} + v_p^\nu)(v_p^{\nu+1} - v_p^\nu) = -\sum_i \epsilon_0 \frac{E^{n+1} - E^n}{\Delta t}\frac{E_i^{n+1} + E_i^n}{2}$$

$$\Rightarrow \boxed{\sum_p \frac{1}{2} m_p v_p^2 + \sum_i \frac{1}{2}\epsilon_0 E_i^2 = \text{const.}}$$

Ion acoustic standing wave: Accuracy impact of manifold preservation

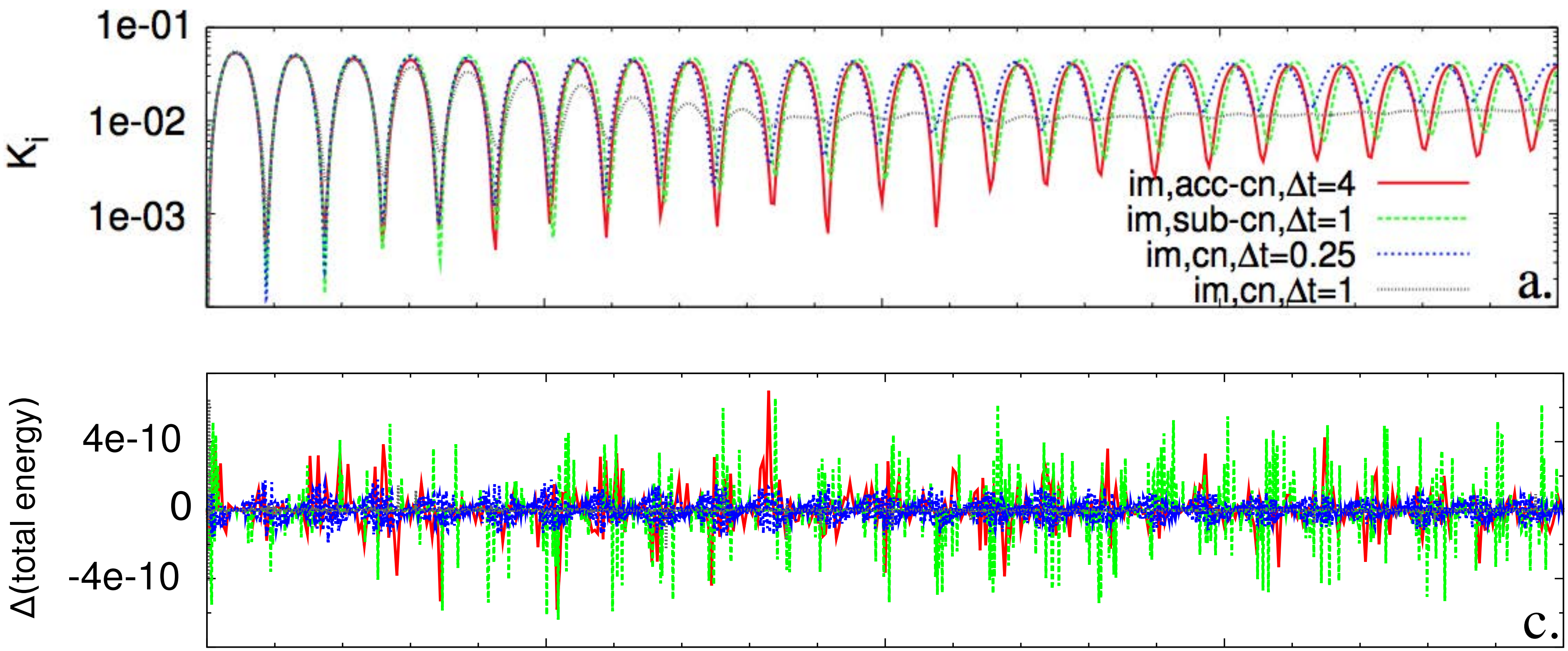

Ion acoustic oscillations

im=implicit

cn=Crank-Nicolson,

sub=fixed-substepping

acc=adaptive charge conserving.

Ion acoustic shock wave: Accuracy impact of manifold preservation

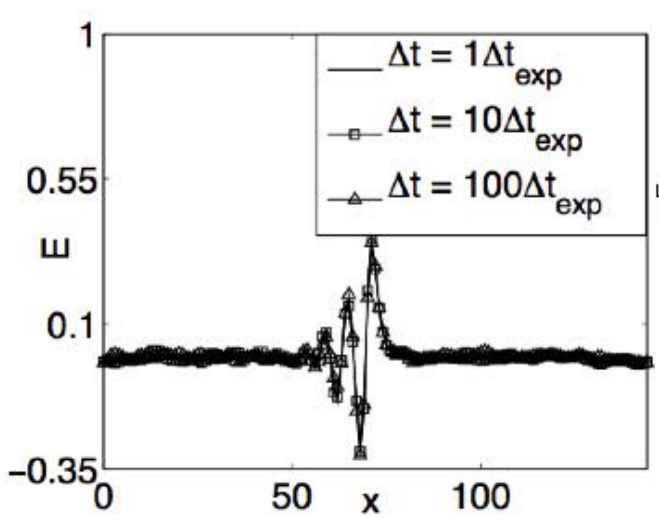

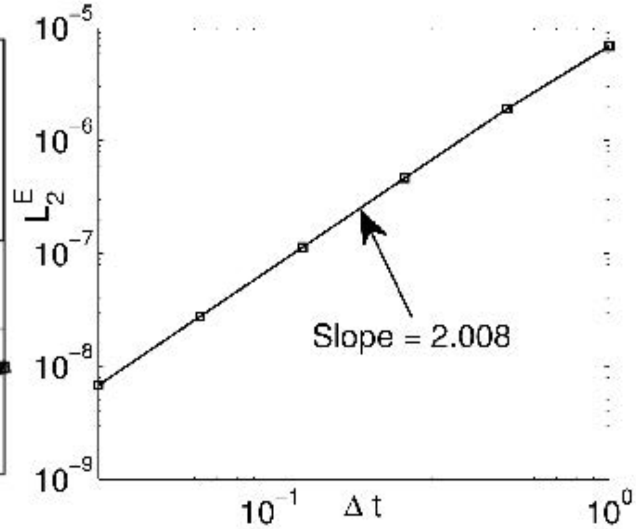

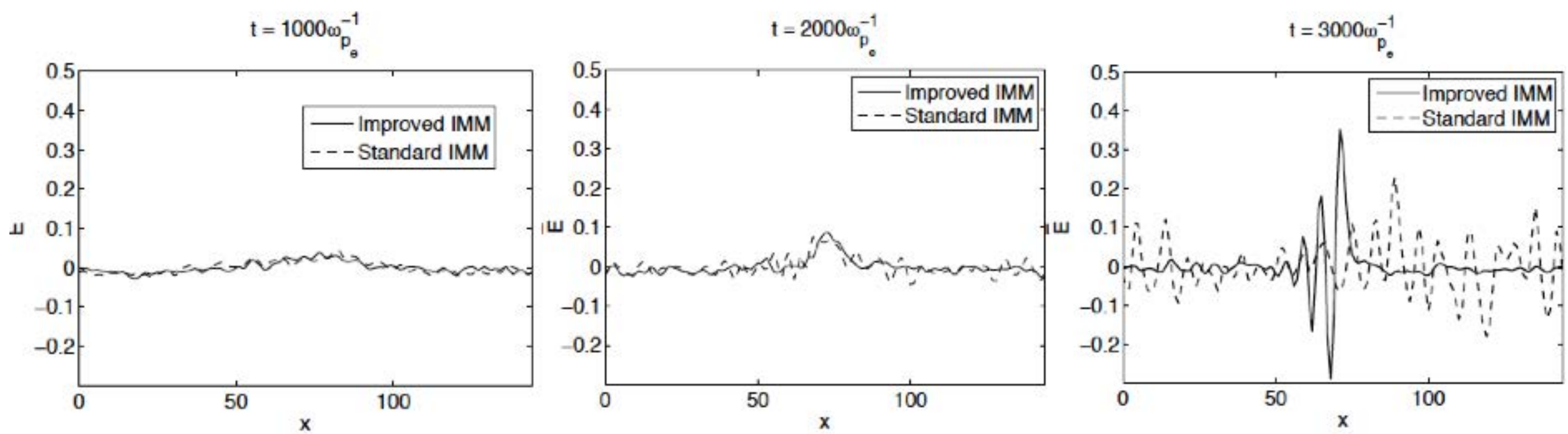

[5] Taitano et al., *SISC*, 35 (2013)

Ion acoustic shock wave:
Long-term accuracy on non-uniform mapped meshes

non-uniform grid spacing

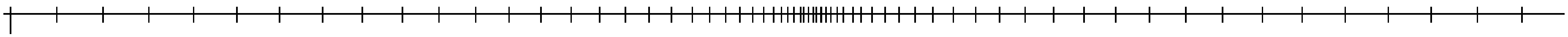

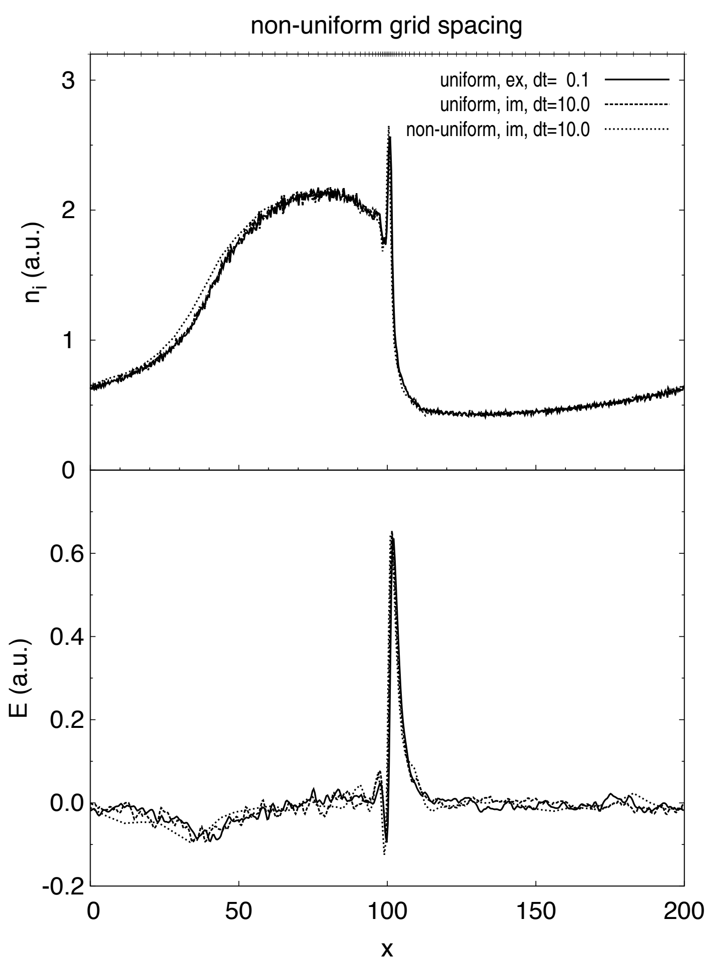

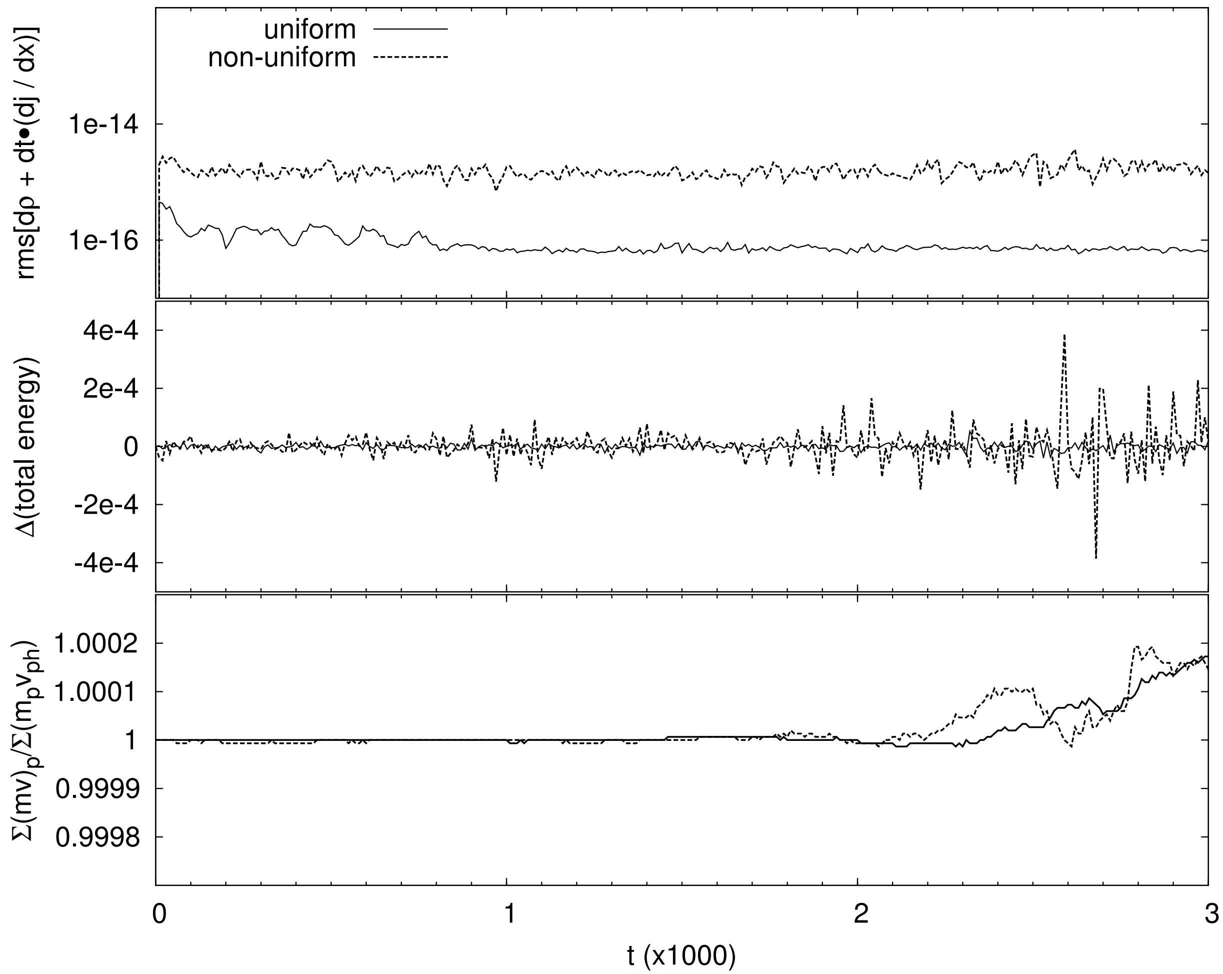

Moment-based preconditioning

Chen et al, JCP 2014; CPC 2014, 2015

CPU gain potential of implicit PIC vs explicit PIC

- Back-of-the-envelope estimate of CPU gain:

$$CPU \sim \left(\frac{T}{\Delta t}\right)\left(\frac{L}{\Delta x}\right)^d n_p C^{solver} \quad ; \quad \frac{C^{imp}}{C^{ex}} \sim N_{FE}\frac{\Delta t_{imp}}{\Delta \tau_{imp}} \quad ; \quad \frac{CPU_{ex}}{CPU_{imp}} \sim \left(\frac{\Delta x_{imp}}{\Delta x_{ex}}\right)^d \frac{\Delta \tau_{imp}}{\Delta t_{ex}}\frac{1}{N_{FE}}$$

- Using reasonable estimates:

$$\begin{aligned}
\Delta \tau_{imp} &\sim \min\left[0.1\frac{\Delta x_{imp}}{v_{th}}, \Delta t_{imp}\right] \\
{\color{red}\Delta t_{imp}} &\,{\color{red}\sim}\, {\color{red}0.1\omega_{pi}^{-1}} \\
\Delta t_{exp} &\sim 0.1\omega_{pe}^{-1} \\
k\Delta x_{imp} &\sim 0.2 \\
\Delta x_{ex} &\sim \lambda_D
\end{aligned}$$

$$\boxed{\frac{CPU_{ex}}{CPU_{imp}} \sim \left(\frac{L}{\lambda_D}\right)^d \min\left[\frac{L}{\lambda_D}, \sqrt{\frac{m_i}{m_e}}\right]\frac{1}{N_{FE}}}$$

- CPU speedup is:
  - Better for realistic mass ratios and increased dimensionality!
  - Limited by solver performance N_{FE} (preconditioning!)

Moment-based acceleration of fully kinetic algorithm

- Particle elimination $\Rightarrow$ nonlinear residual is formulated in terms of fields/moments ONLY: $\mathbf{F}(E)$
- Within JFNK, preconditioner ONLY needs to provide field/moment update:

$$\boxed{\delta E \approx -P^{-1}\mathbf{F}}$$

> Premise of acceleration: obtain δE from a fluid model using current particle distribution for closure.

- We posit a fluid nonlinear model:

$$\begin{aligned}
\partial_t n_\alpha &= -\nabla \cdot \mathbf{\Gamma}_\alpha \\
m_\alpha \left[\partial_t \mathbf{\Gamma}_\alpha + \nabla \cdot \left(\frac{1}{n_\alpha}\mathbf{\Gamma}_\alpha \mathbf{\Gamma}_\alpha\right)\right] &= q_\alpha n_\alpha \mathbf{E} + \nabla \cdot \left(n_\alpha \left(\frac{\mathbf{\Pi}_\alpha}{n_\alpha}\right)_p\right) \\
\epsilon_0 \partial_t \mathbf{E} &= \sum_\alpha q_\alpha \mathbf{\Gamma}_\alpha
\end{aligned}$$

Moment-based acceleration of fully kinetic alg. (cont.)

- We formulate *approximate* linearized fluid equations (neglect linear temperature response):

$$\begin{aligned}
\frac{\delta n_\alpha}{\Delta t} &= -\nabla \cdot \delta \mathbf{\Gamma}_\alpha \\
m_\alpha \frac{\delta \mathbf{\Gamma}_\alpha}{\Delta t} &\approx q_\alpha (\delta n_\alpha \mathbf{E} + n_{\alpha,p} \delta \mathbf{E}) + \nabla \cdot \left(\left(\frac{\mathbf{\Pi}_\alpha}{n_\alpha} \right)_p \delta n_\alpha \right) \\
\epsilon_0 \delta \mathbf{E} &= \Delta t \left[\sum_\alpha q_\alpha \delta \mathbf{\Gamma}_\alpha - \mathbf{F}(\mathbf{E}) \right]
\end{aligned}$$

δE can be obtained from Newton state $\mathbf{E}$, Newton residual $\mathbf{F}(\mathbf{E})$, and particle closures $\mathbf{\Pi}_{\alpha,p}$ and $n_{\alpha,p}$

Moment preconditioner performance

$$\frac{CPU_{ex}}{CPU_{imp}} \sim \left(\frac{L}{\lambda_D}\right)^d \frac{1}{N_{FE}} \min\left[\frac{L}{\lambda_D}, \sqrt{\frac{m_i}{m_e}}\right]$$

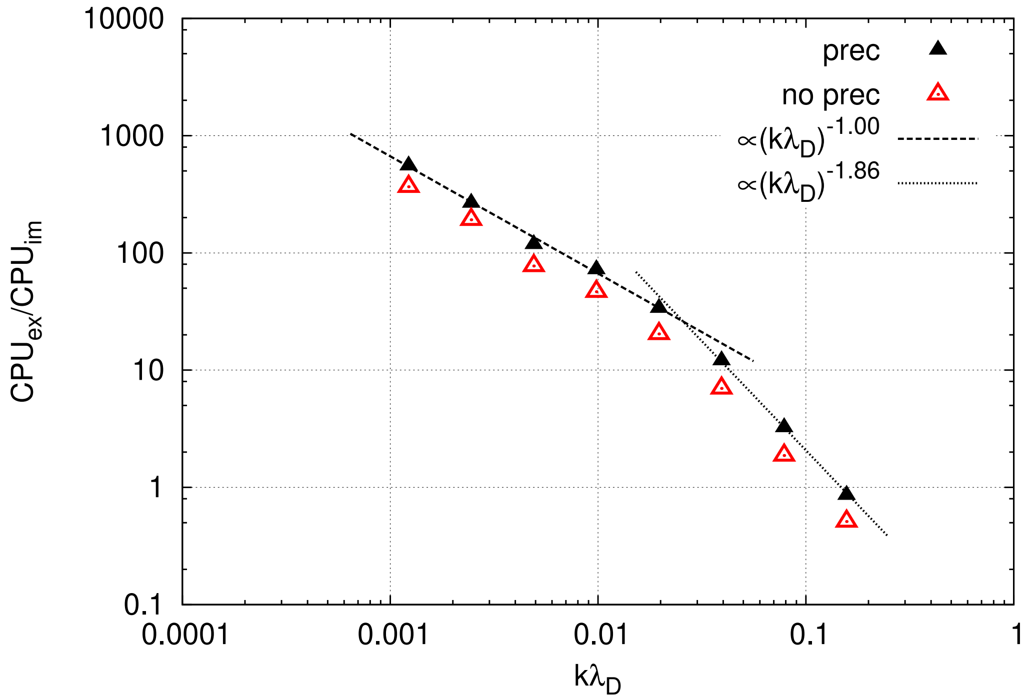

Transition occurs at $k\lambda_D \sim \sqrt{\frac{m_e}{m_i}} \sim 0.025$, as predicted

Extension to multi-D electromagnetic PIC: conservation properties (2D Weibel)

$m_i/m_e = 1836,\ T_{e\perp}/T_{e\parallel} = 9,\ N_{pc}{=}2000,\ L = \pi\, d_e \times \pi\, d_e,\ N_g = 32 \times 32$

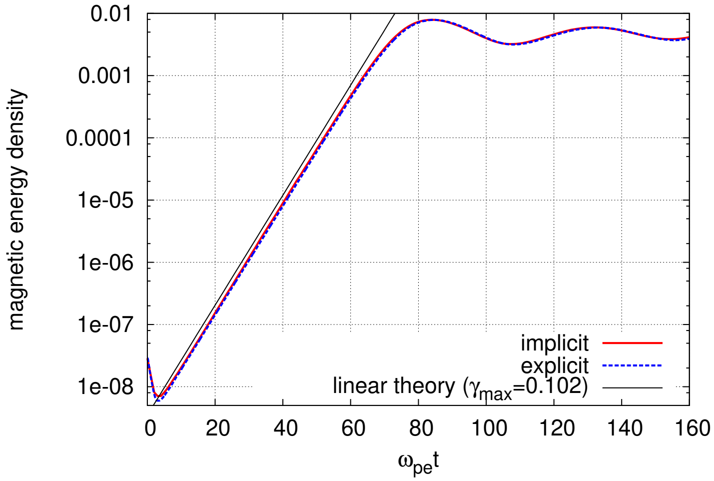

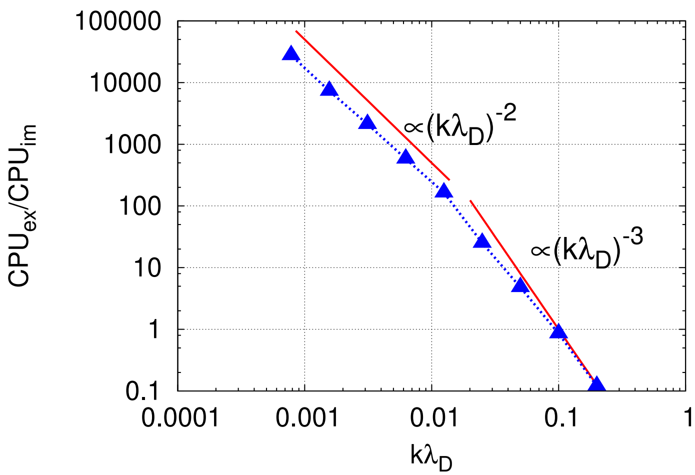

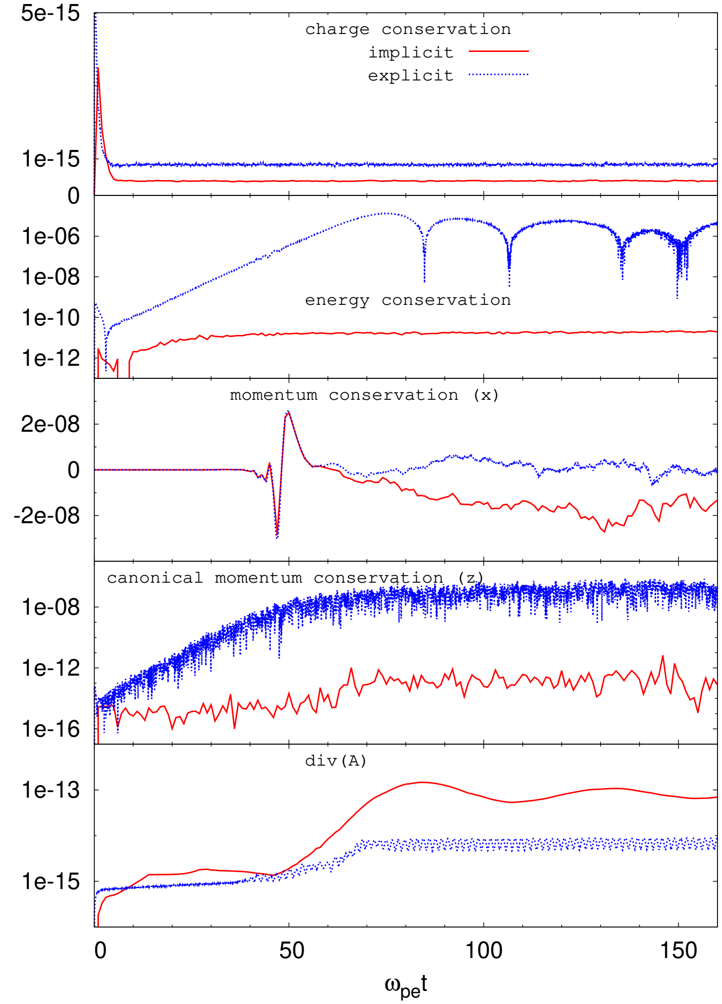

Extension to multi-D electromagnetic PIC: Preconditioner performance (2D Weibel)

$$L_x \times L_y = 22 \times 22 \; (d_e^2), \; N_{pc} = 200, \; \Delta t = 0.1\omega_{pi}^{-1}$$

$$N_x \times N_y = 128 \times 128$$

m_i/m_e	no preconditioner		with preconditioner	
	Newton	GMRES	Newton	GMRES
25	5.8	192.5	3	0
100	5.7	188.8	3	0
1836	7.7	237.8	4	2.8

$$m_i/m_e = 1836$$

$N_x \times N_y$	no preconditioner		with preconditioner	
	Newton	GMRES	Newton	GMRES
16×16	3.7	20	3	0.9
32×32	4	38.5	3	0.9
64×64	4.3	79.9	3	0.2

Manifold-preserving adaptive, implicit Eulerian methods for collisional plasmas

Motivation: Inertial Confinement Fusion (ICF)

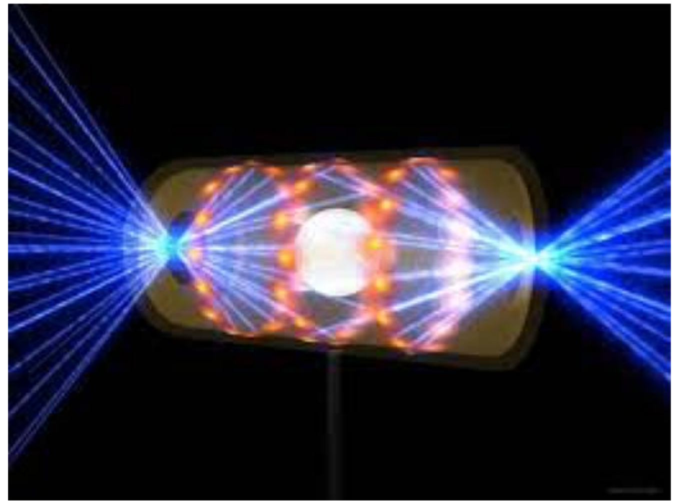

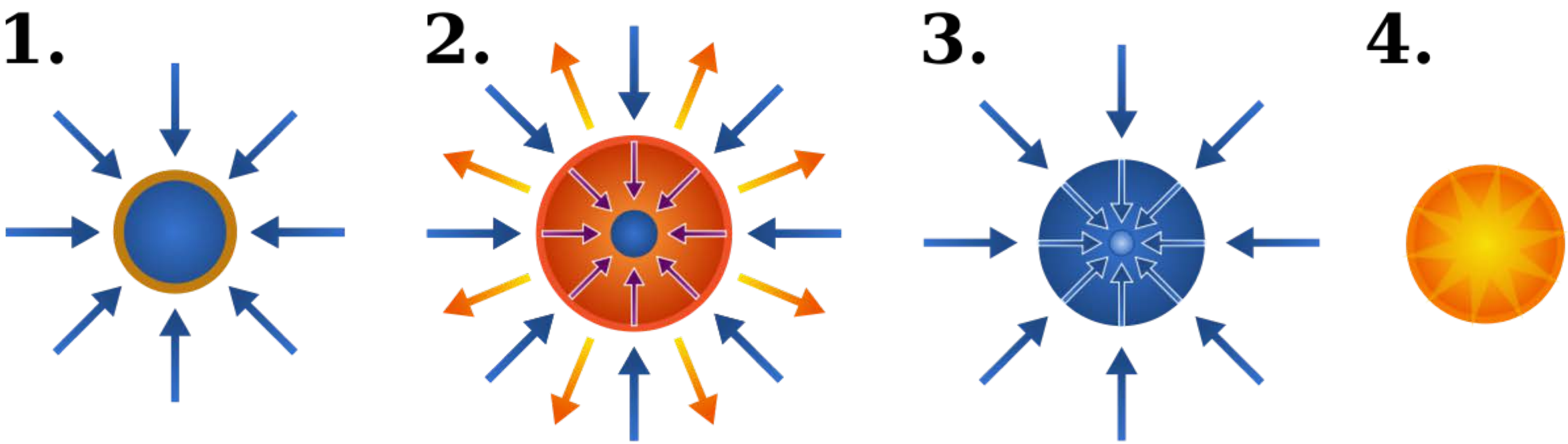

Motivation: Kinetic effects in ICF are important

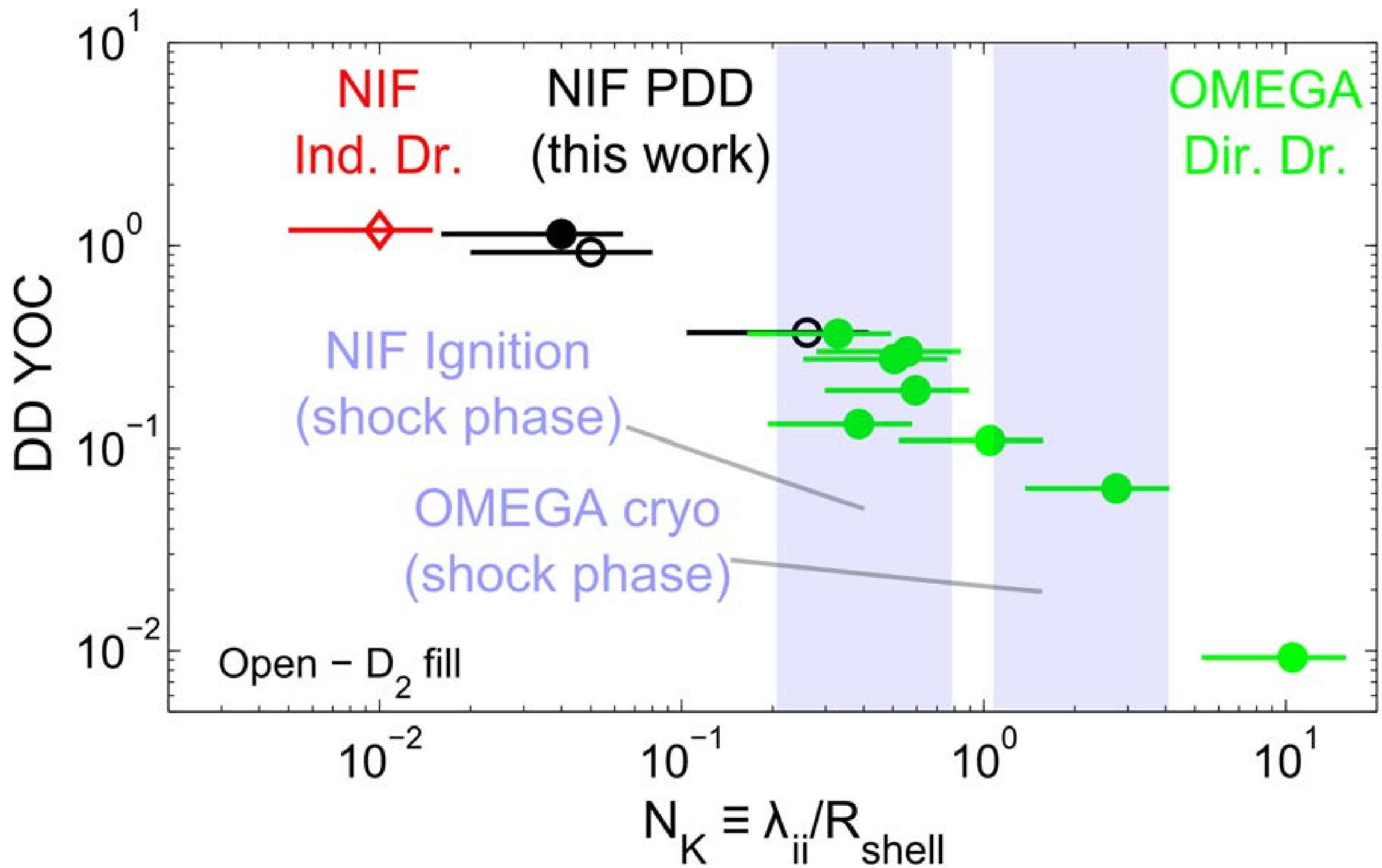

From Rosenberg et al., PoP, **21** (2014)

High-fidelity ICF simulations require a kinetic treatment

- **Vlasov-Fokker-Planck (Rosenbluth form; equivalent to Landau form) is the model of choice for weakly coupled plasmas**

$$\frac{Df_i}{Dt} \equiv \frac{\partial f_i}{\partial t} + \vec{v} \cdot \nabla f_i + \vec{a}_i \cdot \nabla_v f_i = \sum_j \boxed{C_{ij}\left(f_i, f_j\right)}$$

$$\boxed{C_{ij}\left(f_i, f_j\right)} = \Gamma_{ij} \nabla_v \cdot \left[\boxed{D_j} \cdot \nabla_v f_i - \frac{m_i}{m_j} \boxed{A_j} f_i \right]$$

$$\boxed{D_j} = \nabla_v \nabla_v \boxed{G_j} \qquad \boxed{A_j} = \nabla_v \boxed{H_j}$$

$$\nabla_v^2 \boxed{H_j}\left(\vec{v}\right) = -8\pi f_j\left(\vec{v}\right)$$

$$\nabla_v^2 \boxed{G_j}\left(\vec{v}\right) = H_j\left(\vec{v}\right)$$

+ Maxwell's equations…

- **VFP manifold: positivity, conservation of charge, momentum, and energy, H-theorem (entropy increases or stays constant)**

The iFP Vlasov-Fokker-Planck code

Taitano et al, JCP 2015, 2016, 2017, 2018

A multiscale VFP solver for ICF applications

- **Consider 1D-2V geometries (planar, spherical symmetry)**
- **Consider suitable asymptotic limits for Maxwell equations:**
  - Electrostatic approximation (exact in 1D spherical, $\beta \sim 10^3$-10^4 in Omega)
  - Quasineutrality: $\rho = 0$
  - Ambipolarity: $j = 0$ (in 1D)
  - Eliminates plasma frequency, Debye length, and charge separation effects (this is OK for our timescales)
- **Consider fluid electrons:**
  - Rigorous model, including thermal and friction forces (Simakov et al, PoP 2014)
  - Massless electrons (regular limit)
  - Eliminates non-local heat transport effects (drawback)
  - Interim approximation (ambipolarity can be imposed with kinetic e)
- **Ions remain fully kinetic, allow for multiple species**

Model equations:
fully kinetic ions + fluid electrons

Vlasov-Fokker-Planck
for ion species

Fluid electrons

$$\frac{3}{2}\partial_t\left(n_e T_e\right)+\frac{5}{2}\partial_x\left(u_e n_e T_e\right)-u_e\partial_x\left(n_e T_e\right)-\partial_x\kappa_e\partial_x T_e=\sum_\alpha C_{e\alpha}$$

$$n_e=-q_e^{-1}\sum^{N_s} q_\alpha n_\alpha \qquad u_e=-q_e^{-1}n_e^{-1}\sum_{\alpha\neq e}^{N_s} q_\alpha n_\alpha u_\alpha$$

Electric field model: e pressure, friction, thermal forces

$$E=-\frac{\nabla p_e+\sum_i \mathbf{F}_{ie}}{e n_e}=-\frac{\nabla p_e}{e n_e}-\frac{\alpha_0(Z_{eff})m_e}{e}\sum_i \nu_{ei}(\mathbf{V}_e-\mathbf{V}_i)-\frac{\beta_0(Z_{eff})}{e}\nabla T_e$$

Simakov and Molvig, PoP **21** (2014)

Algorithmic innovations of iFP

- **Fully nonlinearly time-implicit ($\Delta t >> \tau_{col}$)**
  - Iterate solution to convergence
  - Based on a nested-model HOLO solver, with optimal multigrid preconditioning
- **Optimal, adaptive grid in phase space**
  - Velocity space: normalize to thermal velocity and shift w/r/t flow velocity per ion species
  - Radial coordinate: Moving mesh partial differential equation (MMPDE)
- **Fully conservative (mass, momentum, and energy)**
  - Mesh motion in phase space built into model analytically, and then discretized (no remapping)
  - Enslavement of error in conservation symmetry into discretization

These strategies save > 14 orders of magnitude in computational complexity vs. “brute-force” algorithms (e.g. static uniform grid + explicit time-integration)

ICF adaptive meshing VFP needs

- Disparate temperatures during implosion dictate velocity resolution.
  - $v_{th,max}$ determines L_v
  - $v_{th,min}$ determines Δv

- Shock width and capsule size dictate physical space resolution

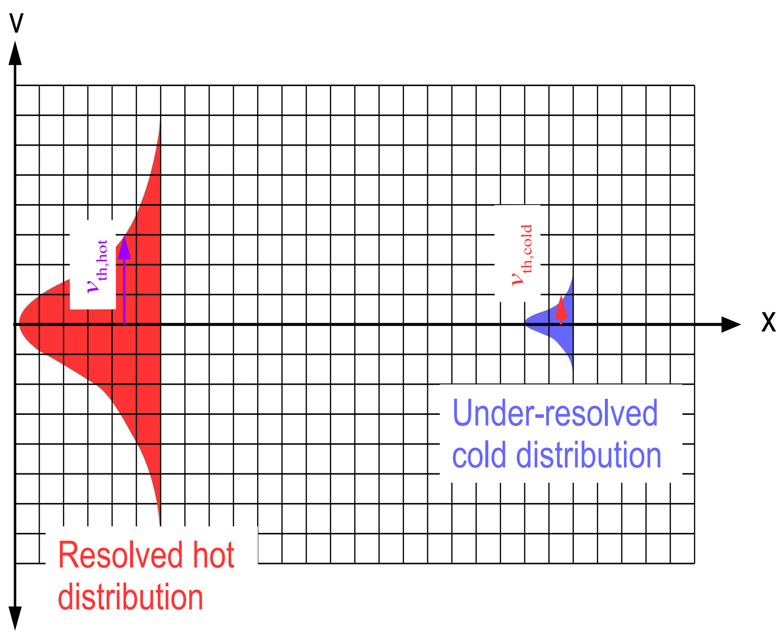

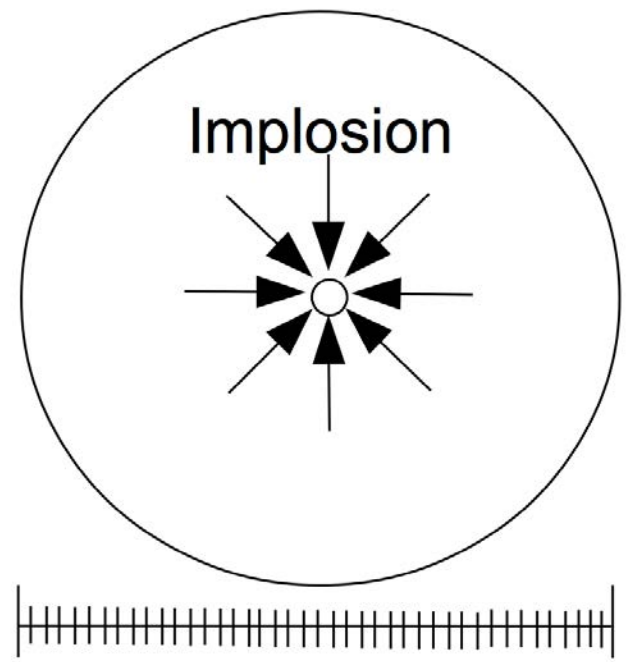

Brute-force VFP algorithms (uniform mesh, explicit timestepping) are impractical for ICF

- **Mesh requirements:**
  - Intra species $v_{th,max} / v_{th,min} \sim 100$
  - Inter species $(v_{th,\alpha} / v_{th,\beta})_{max} \sim 30$
  - $N_v \sim [10(v_{th,max}/v_{th,min}) \times (v_{th,\alpha} / v_{th,\beta})]^2 \sim 10^9$
  - $N_r \sim 10^3 - 10^4$
  - **$N = N_r N_v \sim 10^{12} - 10^{13}$ unknowns in 1D2V!**
- **Timestep requirements:**
  - $t_{sim} = 10$ ns
  - **$N_t = 10^{10}$ time steps**

$$\Delta t_{exp}^{coll} \sim \frac{1}{10} \left(\frac{\Delta v}{v_{th}^{min}} \right)^2 \nu_{coll}^{-1} \sim 10^{-9}\, ns$$

- **Beyond exascale (10^{18} FLOPS)!**

Adaptive mesh with implicit timestepping makes problem tractable

- **Mesh requirements:** $\hat{v} = (v - u_{||})/v_{th}$
  - v-space adaptivity with v_{th} normalization and $u_{||}$ shift, $N_v \sim 10^4 - 10^5$
  - Moving mesh in physical space, $N_r \sim 10^2$
  - Second-order accurate phase-space discretization
  - **$N = N_v N_r \sim 10^6 \sim 10^7$** (vs. 10^{12} with static mesh)
- **Timestep requirements:**
  - Optimal $O(N_v)$ implicit nonlinear algorithms [Chacon, *JCP*, 157 (2000), Taitano et al., *JCP*, 297 (2015)]
  - Second-order-accurate timestepping
  - $\Delta t_{imp} = \Delta t_{str} \sim 10^{-3}$ ns
  - **$N_t \sim 10^3 - 10^4$** (vs. 10^{10} with explicit methods)
- **Terascale-ready! (10^{12} FLOPS, any reasonable cluster)**

v_{th} adaptivity provides an enabling capability to simulate ICF plasmas

- **D-e-α, 3 species thermalization problem**
- **Resolution with static grid:**

$$N_v \sim 2\left(\frac{v_{th,e,\infty}}{v_{th,D,0}}\right)^2 = 140000 \times 70000$$

- **Resolution with adaptivity and asymptotics:**

$$N_v = 128 \times 64$$

- **Mesh savings of**

$$\sim 10^6$$

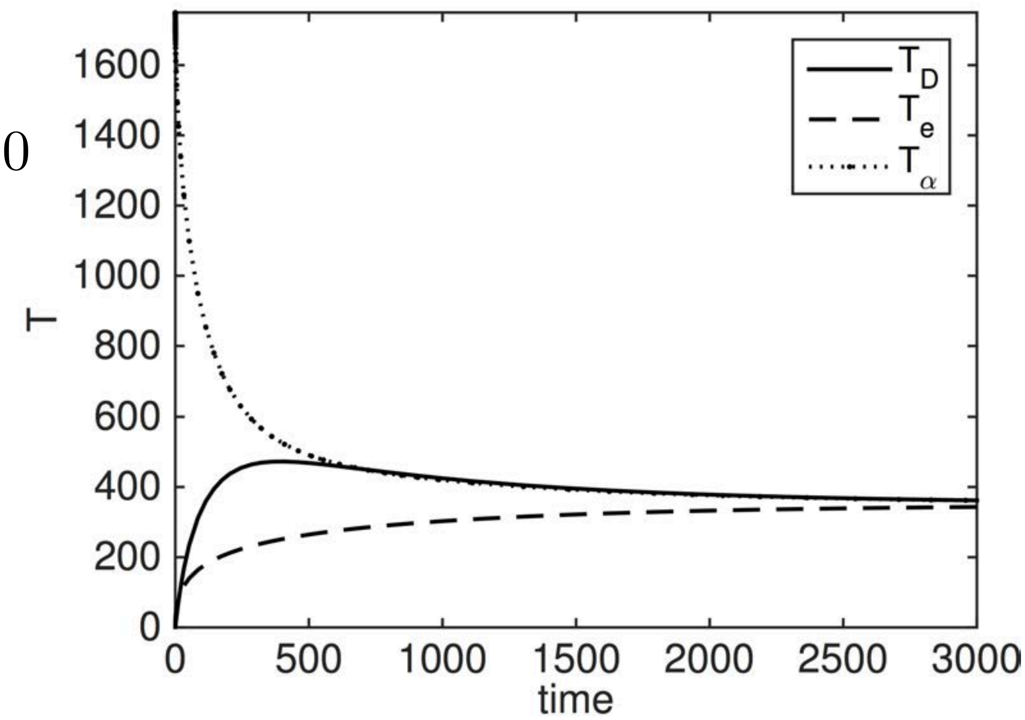

Manifold preservation is critical!

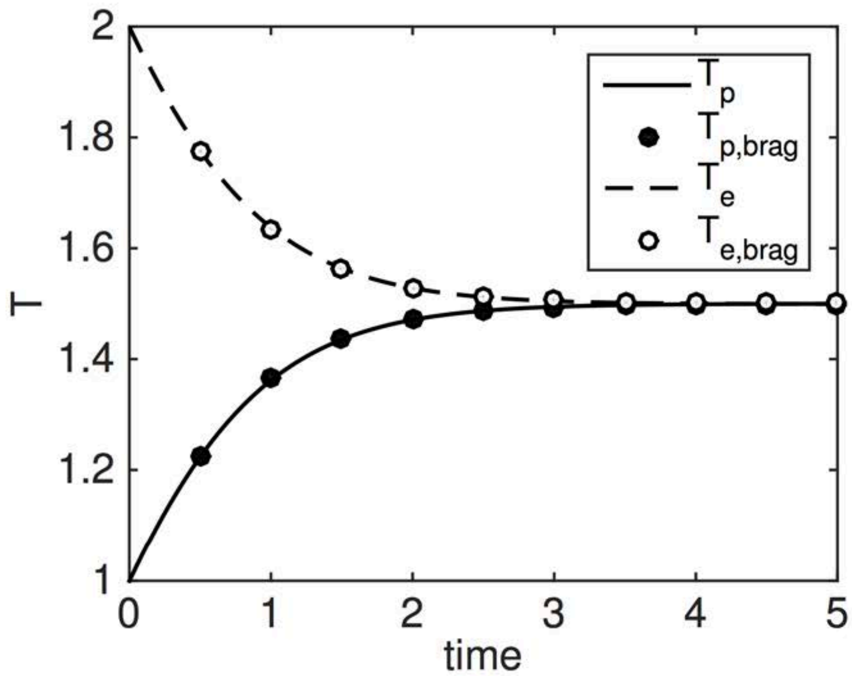

With energy conservation

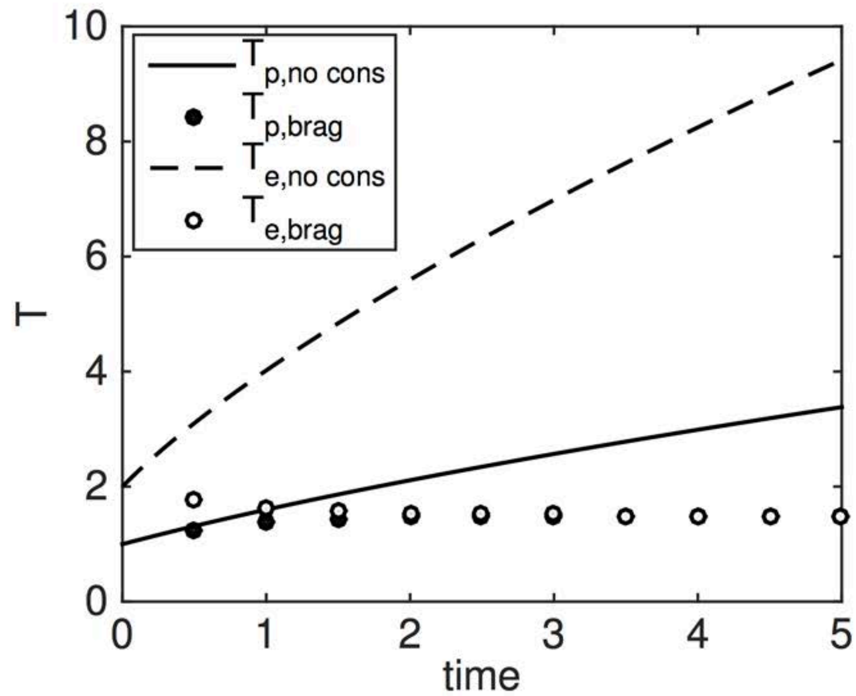

Without energy conservation

Implicit solver is very efficient, algorithmically and in parallel

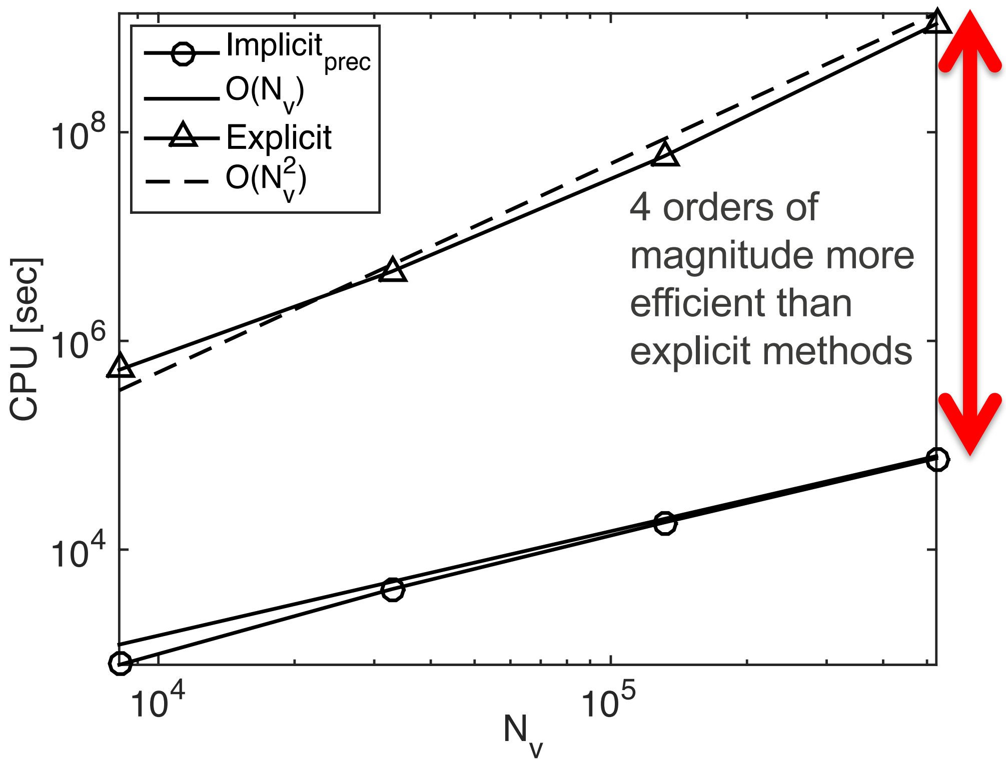

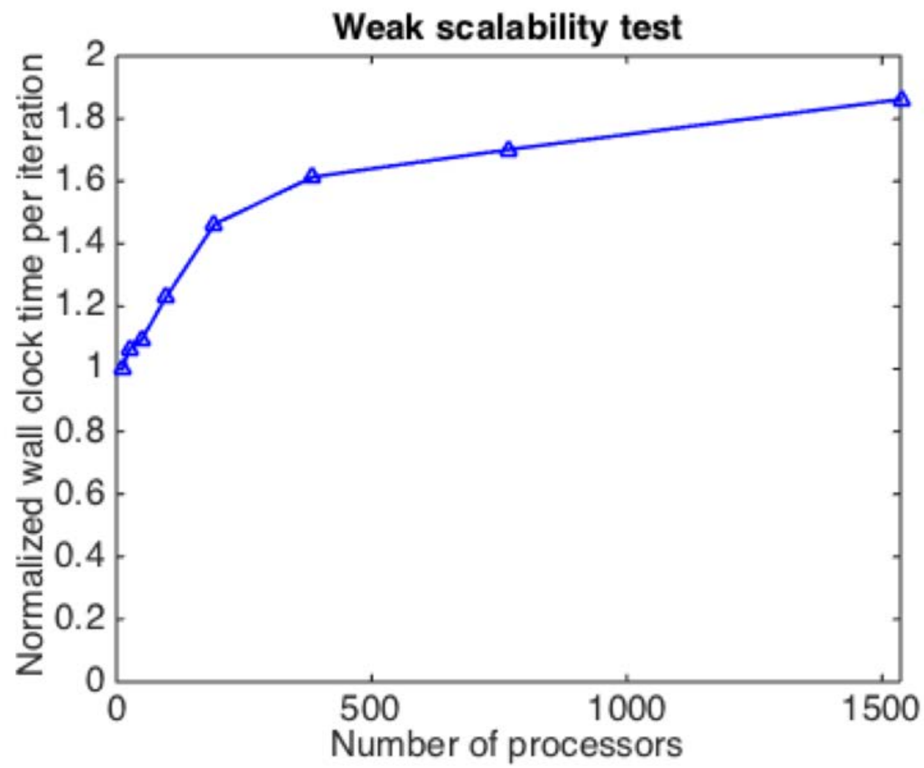

Algorithm achieves design accuracy (2nd order in phase space and temporally)

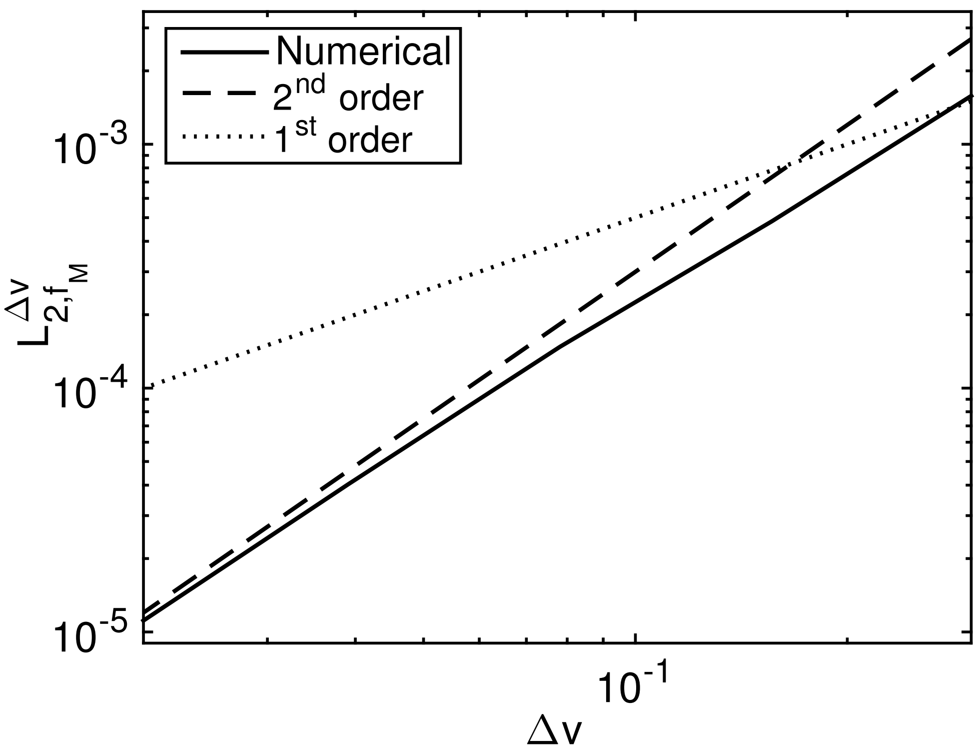

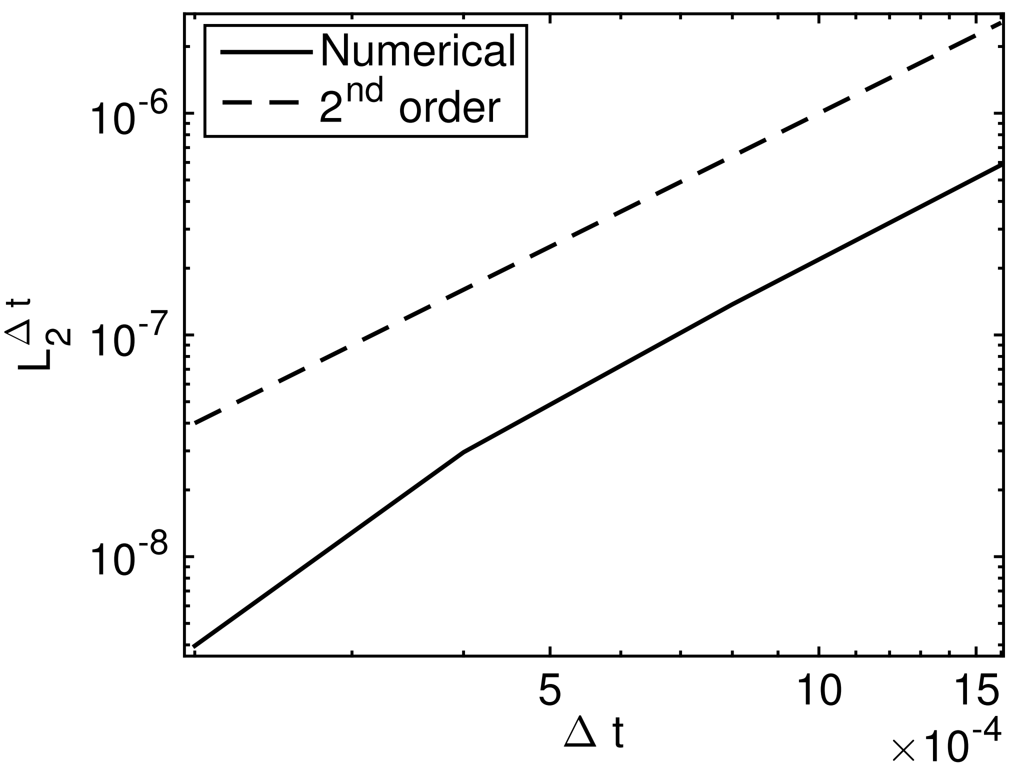

Phase-space **mesh adaptivity** strategy

Taitano et al, JCP 2016, 2017, 2018

1D-2V Rosenbluth-VFP model: Adaptive velocity-space mesh

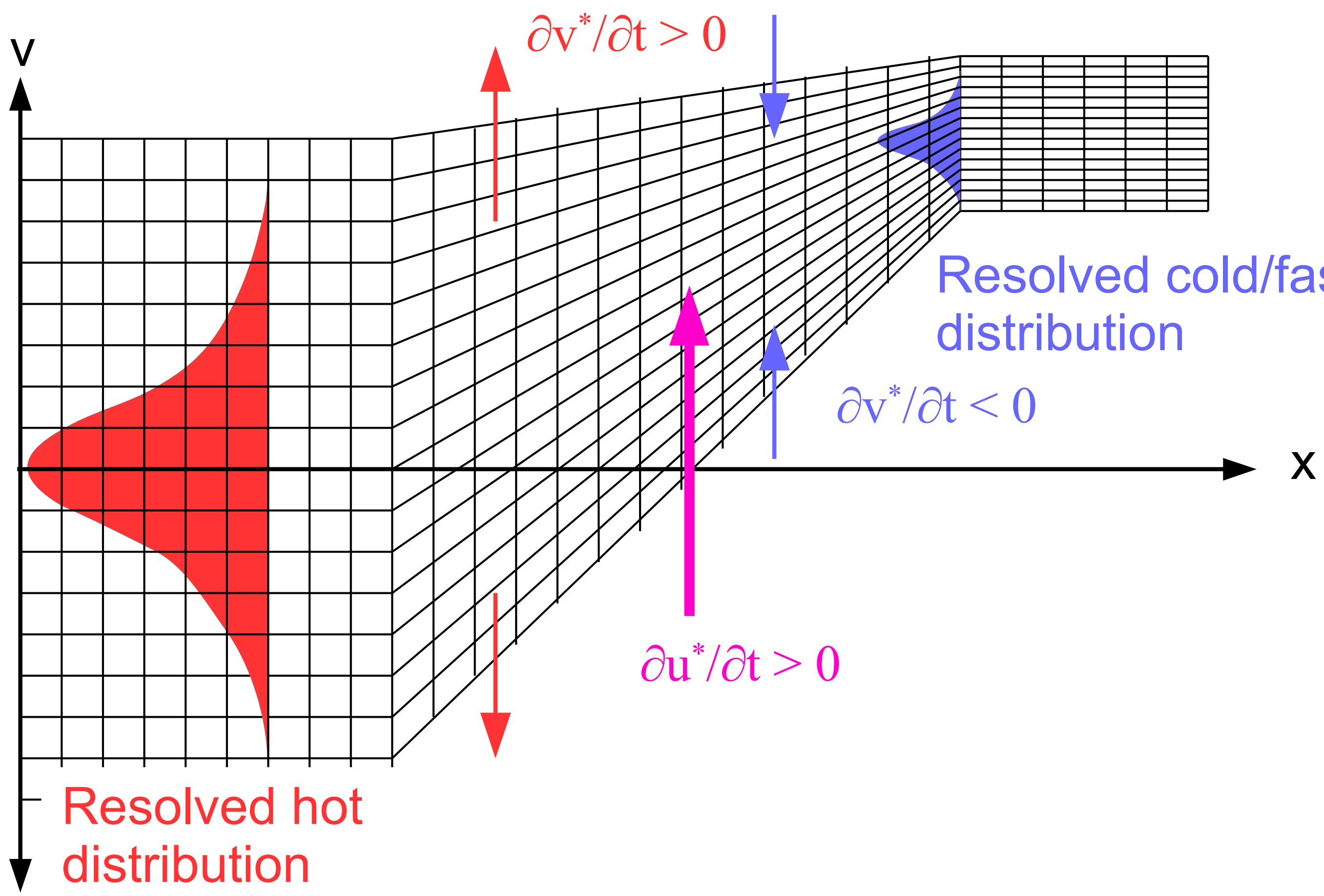

- ➤V-space adaptivity allows optimal mesh resolution throughout the domain
- ➤Analytical transformation introduces inertial terms

Representation and analytical coordinate transformation for v_{th} adaptive meshing

1D spherical (with logical mesh); 2D cylindrical geometry in velocity space

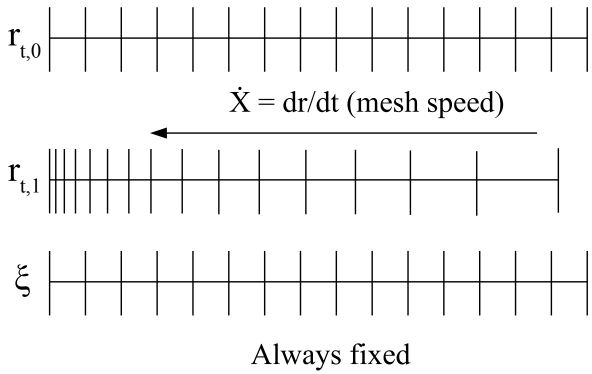

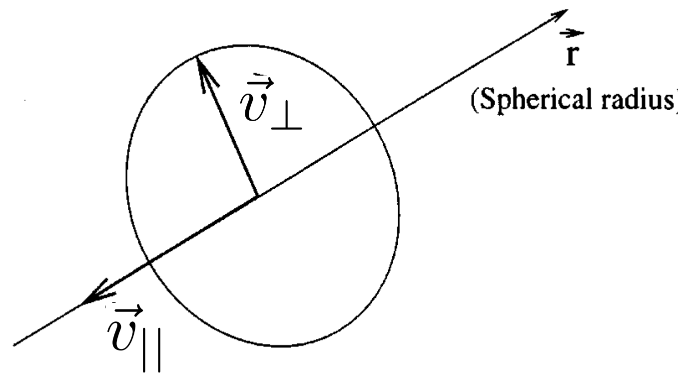

Coordinate transformation:

$$\widehat{v}_{||} \equiv \frac{\vec{v} \cdot \widehat{\vec{r}}}{\boxed{v_{th,\alpha}}}, \quad \widehat{v}_\perp \equiv \frac{\sqrt{v^2 - v_{||}^2}}{\boxed{v_{th,\alpha}}}$$

Jacobian of transformation:

$$\sqrt{g_v}\,(t, r, \widehat{v}_\perp) \equiv v_{th,\alpha}^3\,(t, r)\, r^2 \widehat{v}_\perp$$

$$J_{r\xi} = \partial_\xi r$$

Coordinate transformation introduces inertial terms

➤**VRFP equation in transformed coordinates**

$$\partial_t \left(\sqrt{g_v} J_{r\xi} f_\alpha\right) + \partial_\xi \left(\sqrt{g_v} v_{th,\alpha} \left[\widehat{v}_{||} - \boxed{\widehat{\dot{r}}_\alpha}\right] f_\alpha\right) +$$

$$\partial_{\widehat{v}_{||}} \left(J_{r\xi}\sqrt{g_v} \boxed{\widehat{\dot{v}}_{||}} f_\alpha\right) + \partial_{\widehat{v}_\perp} \left(J_{r\xi}\sqrt{g_v} \boxed{\widehat{\dot{v}}_\perp} f_\alpha\right) = J_{r\xi}\sqrt{g_v} \sum_\beta^{N_s} C_{\alpha\beta}\left(f_\alpha, f_\beta\right)$$

$$\boxed{\widehat{\dot{v}}_{||}} = -\boxed{\frac{\widehat{v}_{||}}{2}\left(v_{th,\alpha}^{-2}\partial_t v_{th,\alpha}^2 + J_{r\xi}^{-1}\left(\widehat{v}_{||} - \widehat{\dot{x}}\right) v_{th,\alpha}^{-1}\partial_\xi v_{th,\alpha}^2\right)} + \frac{\widehat{v}_\perp^2 v_{th,\alpha}}{r} + \frac{q_\alpha E_{||}}{J_{r\xi} m_\alpha v_{th,\alpha}}$$

$$\boxed{\widehat{\dot{v}}_\perp} = -\boxed{\frac{\widehat{v}_\perp}{2}\left(v_{th,\alpha}^{-2}\partial_t v_{th,\alpha}^2 + J_{r\xi}^{-1}\left(\widehat{v}_{||} - \widehat{\dot{x}}\right) v_{th,\alpha}^{-1}\partial_\xi v_{th,\alpha}^2\right)} - \frac{\widehat{v}_{||}\widehat{v}_\perp v_{th,\alpha}}{r}$$

Collision operator:
Asymptotic treatment of interspecies collisions

Taitano et al, JCP 2016

Interspecies collisions present challenges with species-centric mesh adaption

- **Adaptivity using v_{th} requires solving the interspecies collision problem: one needs to compute the potentials for species β on the mesh of species α**

$$\boxed{\widehat{C}_{\alpha\beta} = \frac{\Gamma_{\alpha\beta}}{v_{th,\beta}^3}\widehat{\nabla}_{v_\alpha}\cdot\left[\widehat{\nabla}_{v_\alpha}\widehat{\nabla}_{v_\alpha}\widehat{G}_{\alpha\beta}\cdot\widehat{\nabla}_{v_\alpha}\widehat{f}_\alpha - \frac{m_\alpha}{m_\beta}\widehat{f}_\alpha\widehat{\nabla}_{v_\alpha}\widehat{H}_{\alpha\beta}\right]}$$

$$\widehat{\nabla}^2_{v_\alpha}\widehat{H}_{\alpha\beta} = -8\pi\,\boxed{\widehat{f}_\beta\left(\widehat{v}_\beta = \widehat{v}_\alpha\frac{v_{th,\alpha}}{v_{th,\beta}}\right)} \qquad \widehat{\nabla}^2_{v_\alpha}\widehat{G}_{\alpha\beta} = \widehat{H}_{\alpha\beta}$$

$$\hat{H}_{\alpha\beta} = H_\beta\frac{v_{th,\beta}^3}{v_{th,\alpha}^2} \qquad \hat{G}_{\alpha\beta} = G_\beta\frac{v_{th,\beta}^3}{v_{th,\alpha}^4}$$

- **This transfer can be problematic:**
  - Accuracy issues (when species have disparate thermal velocities)
  - Efficiency issues: work scales as number of species squared $O(N_s^2)$
- **Asymptotic treatment solves both issues**

Asymptotic Formulation of Interspecies Collisions

$v_f/v_{th,s} >> 1$

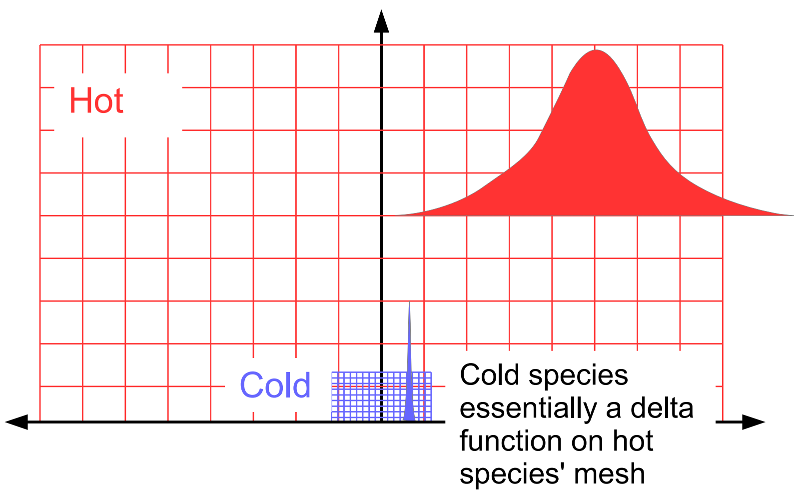

$$H_s = \frac{n_s}{v} + \frac{n_s \boldsymbol{V}_s \cdot \boldsymbol{v}}{v^3} + \cdots$$

$$G_s = n_s v - \frac{n_s \boldsymbol{V}_s \cdot \boldsymbol{v}}{v} + \boldsymbol{\nabla}_v \boldsymbol{\nabla}_v v : \left(\frac{1}{2} \int \mathrm{d}^3 v' \, f_s' \boldsymbol{v}' \boldsymbol{v}' \right) + \cdots$$

$v_s/v_{th,f} << 1$

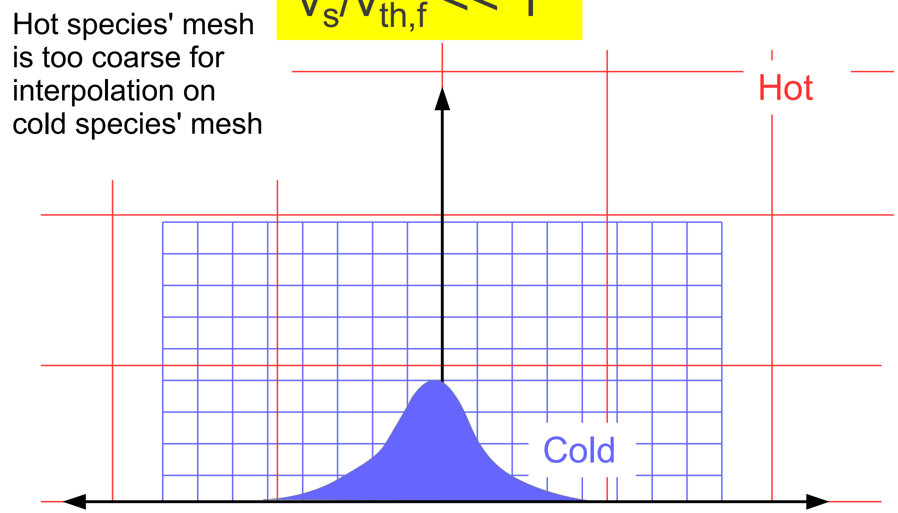

$$\begin{aligned} H_f = \boldsymbol{v} \cdot \left(\int \mathrm{d}^3 v' \, f_f' \frac{\boldsymbol{v}'}{v'^3} \right) &+ \frac{1}{2} \boldsymbol{v}\boldsymbol{v} : \left[\int \mathrm{d}^3 v' \, f_f' \boldsymbol{\nabla}_{v'} \boldsymbol{\nabla}_{v'} \left(\frac{1}{v'} \right) \right] \\ &- \frac{1}{6} \boldsymbol{v}\boldsymbol{v}\boldsymbol{v} \vdots \left[\int \mathrm{d}^3 v' \, f_f' \boldsymbol{\nabla}_{v'} \boldsymbol{\nabla}_{v'} \boldsymbol{\nabla}_{v'} \left(\frac{1}{v'} \right) \right] \\ &+ \frac{1}{24} \boldsymbol{v}\boldsymbol{v}\boldsymbol{v}\boldsymbol{v} :: \left[\int \mathrm{d}^3 v' \, f_f' \boldsymbol{\nabla}_{v'} \boldsymbol{\nabla}_{v'} \boldsymbol{\nabla}_{v'} \boldsymbol{\nabla}_{v'} \left(\frac{1}{v'} \right) \right] + \cdots \end{aligned}$$

$$\begin{aligned} G_f = \frac{1}{2} \boldsymbol{v}\boldsymbol{v} : \left(\int \mathrm{d}^3 v' \, f_f' \boldsymbol{\nabla}_{v'} \boldsymbol{\nabla}_{v'} v' \right) &- \frac{1}{6} \boldsymbol{v}\boldsymbol{v}\boldsymbol{v} \vdots \left(\int \mathrm{d}^3 v' \, f_f' \boldsymbol{\nabla}_{v'} \boldsymbol{\nabla}_{v'} \boldsymbol{\nabla}_{v'} v' \right) \\ &+ \frac{1}{24} \boldsymbol{v}\boldsymbol{v}\boldsymbol{v}\boldsymbol{v} :: \left(\int \mathrm{d}^3 v' \, f_f' \boldsymbol{\nabla}_{v'} \boldsymbol{\nabla}_{v'} \boldsymbol{\nabla}_{v'} \boldsymbol{\nabla}_{v'} v' \right) + \cdots \end{aligned}$$

v_{th} adaptivity provides an enabling capability to simulate ICF plasmas

- D-e-α, 3 species thermalization problem
- Resolution with static grid:

$$N_v \sim 2\left(\frac{v_{th,e,\infty}}{v_{th,D,0}}\right)^2 = 140000 \times 70000$$

- Resolution with adaptivity and asymptotics:

$$N_v = 128 \times 64$$

- Mesh savings of

$$\sim 10^6$$

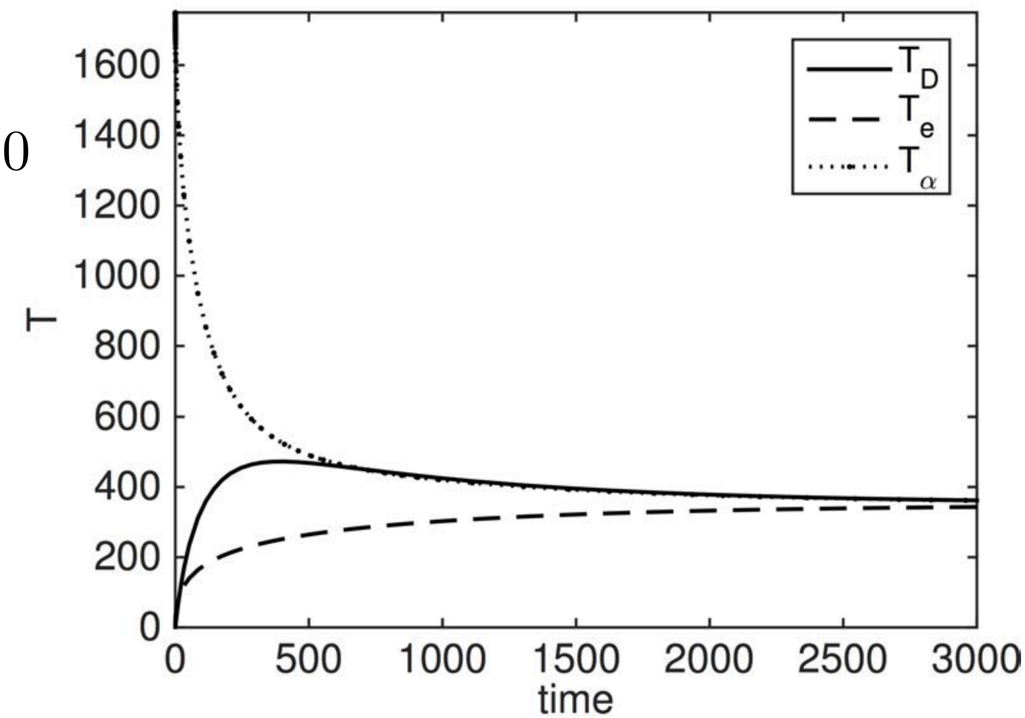

Collision operator:
Conservation and positivity

2V Rosenbluth-FP collision operator: conservation symmetries

➤ **Conservation properties of FP collision operator result from symmetries:**

$$C_{\alpha\beta} = \Gamma_{\alpha\beta} \nabla_v \cdot \left[\vec{J}_{\alpha\beta,G} - \frac{m_\alpha}{m_\beta} \vec{J}_{\alpha\beta,H} \right]$$

Mass

$$\langle 1, C_{\alpha\beta} \rangle_{\vec{v}} = 0 \quad \Rightarrow \quad \boxed{\left. \vec{J}_{\alpha\beta,G} - \vec{J}_{\alpha\beta,H} \right|_{\partial\vec{v}} = 0}$$

Momentum

$$m_\alpha \langle \vec{v}, C_{\alpha\beta} \rangle_{\vec{v}} = -m_\beta \langle \vec{v}, C_{\beta\alpha} \rangle_{\vec{v}} \quad \Rightarrow \quad \boxed{\left\langle 1, J^{\|}_{\alpha\beta,G} - J^{\|}_{\beta\alpha,H} \right\rangle_{\vec{v}} = 0}$$

Energy

$$m_\alpha \left\{ \left\langle v^2, C_{\alpha\beta} \right\rangle_{\vec{v}} \right\} = -m_\beta \left\{ \left\langle v^2, C_{\beta\alpha} \right\rangle_{\vec{v}} \right\} \Rightarrow \boxed{\left\langle \vec{v}, \vec{J}_{\beta\alpha,G} - \vec{J}_{\alpha\beta,H} \right\rangle_{\vec{v}} = 0}$$

2V Rosenbluth-FP collision operator: numerical conservation of energy

- The symmetry to enforce is: $\left\langle \vec{v}, \vec{J}_{\beta\alpha,G} - \vec{J}_{\alpha\beta,H} \right\rangle_{\vec{v}} = 0$
- Due to discretization error: $\left\langle \vec{v}, \vec{J}_{\beta\alpha,G} - \vec{J}_{\alpha\beta,H} \right\rangle_{\vec{v}} = \boxed{\mathcal{O}\left(\Delta_v\right)}$
- We introduce a constraint coefficient such that:

$$\left\langle \vec{v}, \boxed{\gamma_{\beta\alpha}} \vec{J}_{\beta\alpha,G} - \vec{J}_{\alpha\beta,H} \right\rangle_{\vec{v}} = 0 \qquad \gamma_{\beta\alpha} = \frac{\left\langle \vec{v}, \vec{J}_{\alpha\beta,H} \right\rangle_{\vec{v}}}{\left\langle \vec{v}, \vec{J}_{\beta\alpha,G} \right\rangle_{\vec{v}}} = 1 + \boxed{\mathcal{O}\left(\Delta_v\right)}$$

$$C_{\alpha\beta} = \Gamma_{\alpha\beta} \nabla_v \cdot \left[\boxed{\gamma_{\alpha\beta}} \vec{J}_{\alpha\beta,G} - \frac{m_\alpha}{m_\beta} \vec{J}_{\alpha\beta,H} \right]$$

- Discretization is nonlinear, and ensures that, numerically:

$$m_\alpha \left\{ \left\langle v^2, C_{\alpha\beta} \right\rangle_{\vec{v}} \right\} = -m_\beta \left\{ \left\langle v^2, C_{\beta\alpha} \right\rangle_{\vec{v}} \right\}$$

- Similarly for momentum. Idea extends to Vlasov equation as well.

2V Rosenbluth-FP collision operator: numerical preservation of positivity

- **RFP collision operator is an advection-(tensor) diffusion operator in velocity space**
- **Use SMART [1] for advection**
  - High-order advection when possible
  - Reverts to upwinding otherwise
  - Monotonic, positivity preserving
  - Suitable for implicit timestepping
- **Use limited tensor diffusion [2,3] for tensor diffusion component**
  - Maximum-principle preserving
  - Compatible with nonlinear iterative solvers

1. Gaskell & Law, 1988
2. Lipnikov et al., 2012
3. Du Toit et al., 2018

Verification: thermalization of initial random distribution

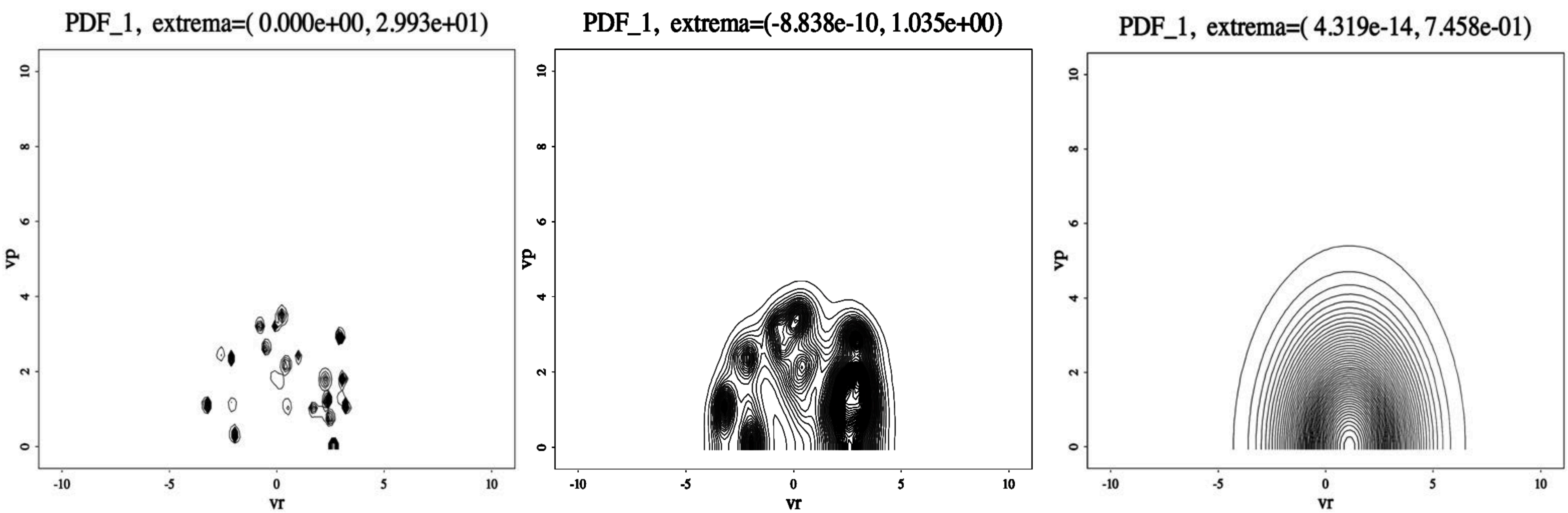

Single-species random distribution: Conservation properties

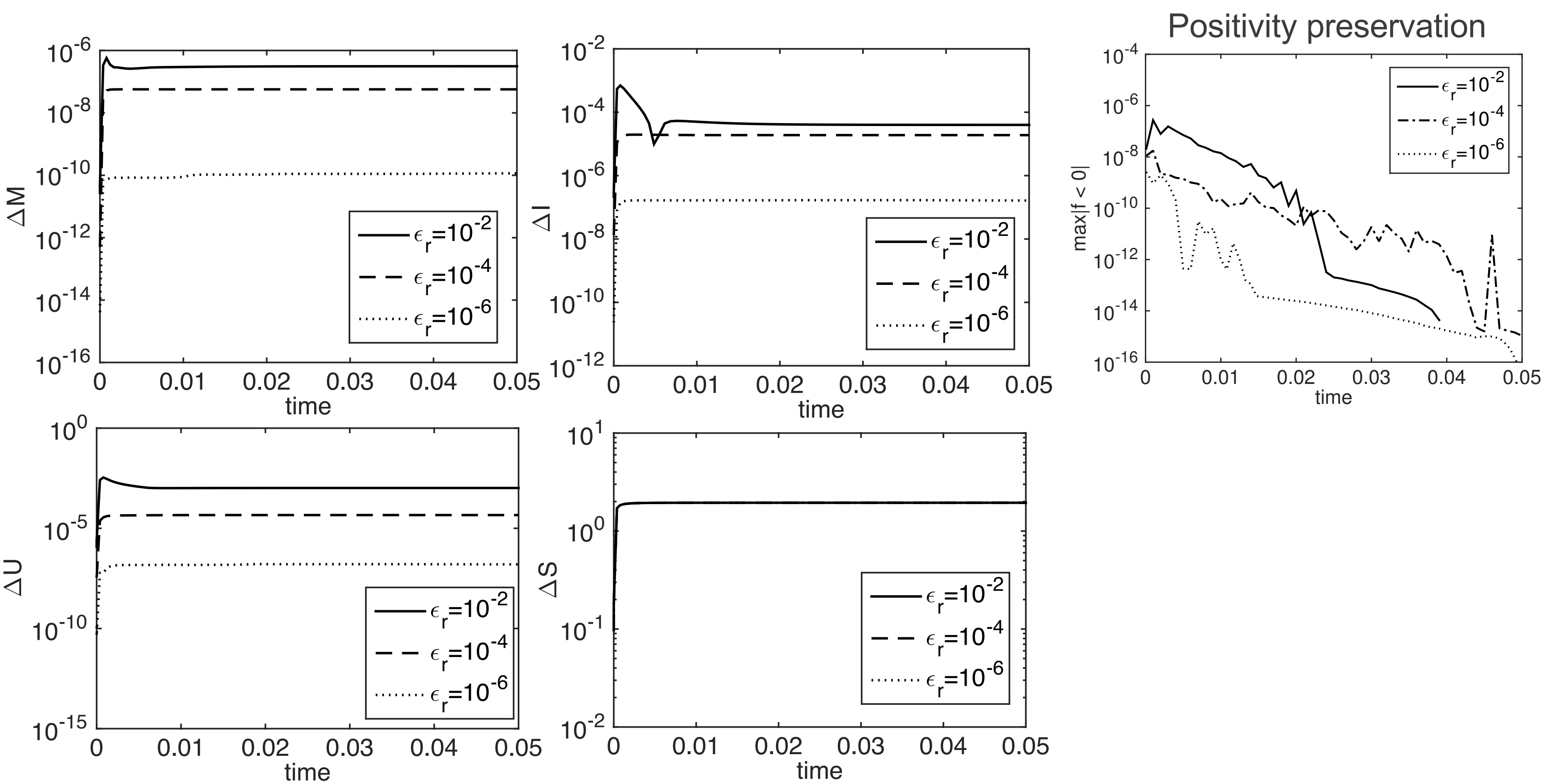

Moment-based (High-Order/Low-Order) nonlinear solver acceleration strategy

Nested-model solver uses the moment equation to efficiently deal with the integral nonlinearity

➤Kinetic (HO) equation (microscopic physics):

$$VFP_\alpha = \partial_t f_\alpha + \nabla_x \cdot (\vec{v} f_\alpha) + (q_\alpha / m_\alpha)\, \vec{E} \cdot \nabla_v f_\alpha - \sum_\beta^N C\left(f_\beta, f_\alpha, n_\beta^{LO}, u_\beta^{LO}, T_\beta^{LO}\right)$$

➤Hydrodynamic (LO) equations (macroscopic physics; evolve the Maxwellian collision kernel):

$$\left\langle \begin{bmatrix} 1 \\ \vec{v} \\ \frac{v^2}{2} \end{bmatrix}, VFP_\alpha \right\rangle_v => \left\{ \begin{array}{c} \partial_t n_\alpha^{LO} + \nabla_x \cdot n\vec{u}_\alpha^{LO} \\ \partial_t n\vec{u}_\alpha^{LO} + \nabla_x \cdot \left[n\vec{u}^{LO} \otimes \vec{u}^{LO} + \bar{I}P^{LO} - \bar{\tau}^{HO} \right] - (q_\alpha/m_\alpha)\, n_\alpha^{LO} \vec{E} + \sum_\beta^N \vec{F}_{\alpha\beta}^{HOLO} \\ \partial_t U_\alpha^{LO} + \nabla_x \cdot \left[\vec{u}^{LO} \left(U_\alpha^{LO} + P_\alpha^{LO} \right) + \vec{Q}_\alpha^{HO} - \vec{u}_\alpha^{LO} \cdot \bar{\tau}_\alpha^{HO} \right] - (q_\alpha/m_\alpha)\, n\vec{u}^{LO} \cdot \vec{E} - \sum_\beta^N W_{\alpha\beta}^{HOLO} \end{array} \right\}$$

➤These systems are **solved coupled** using an accelerated Picard iteration (e.g., Anderson Acceleration)

➤HOLO algorithm effectively **linearizes** the HO component, but without approximation upon nonlinear convergence

LO system accelerates the convergence of the HO system

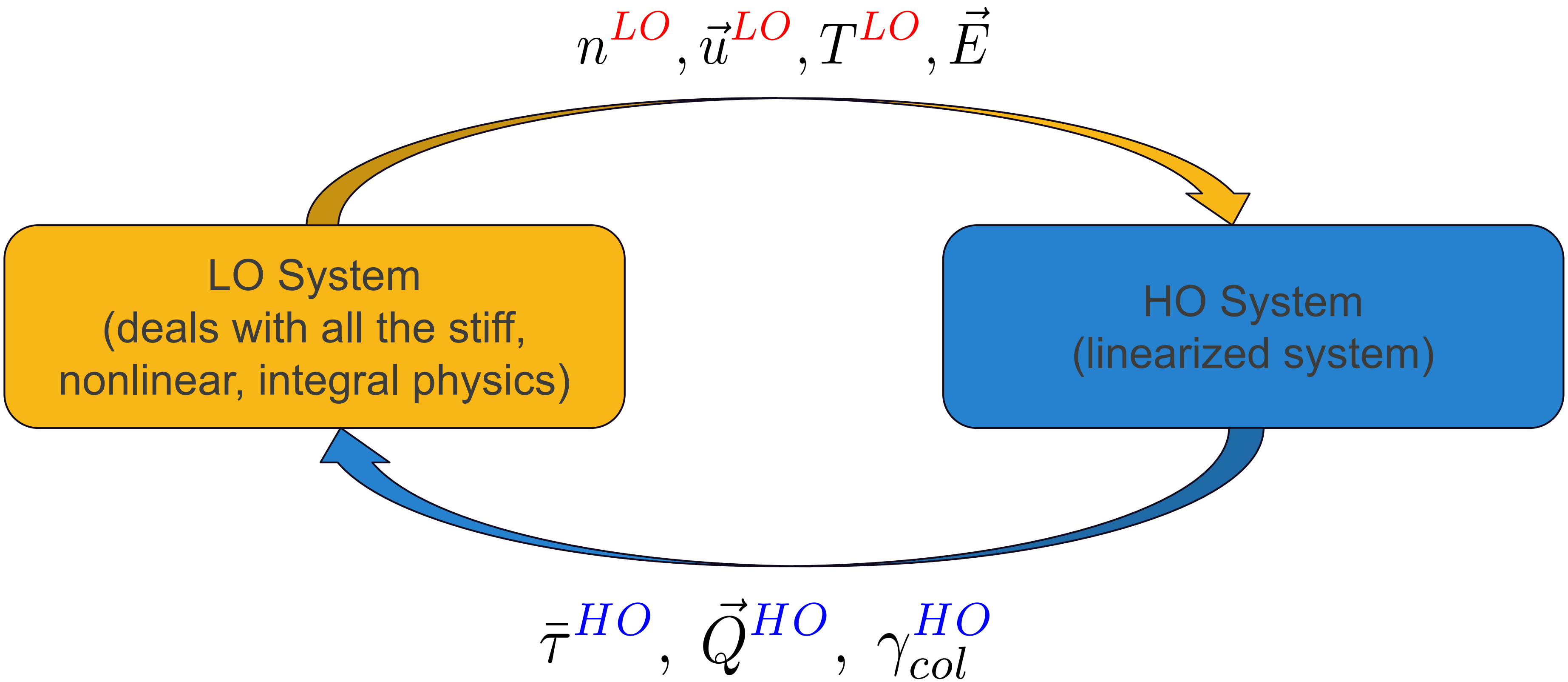

HOLO can efficiently deal with stiff integral nonlinearity

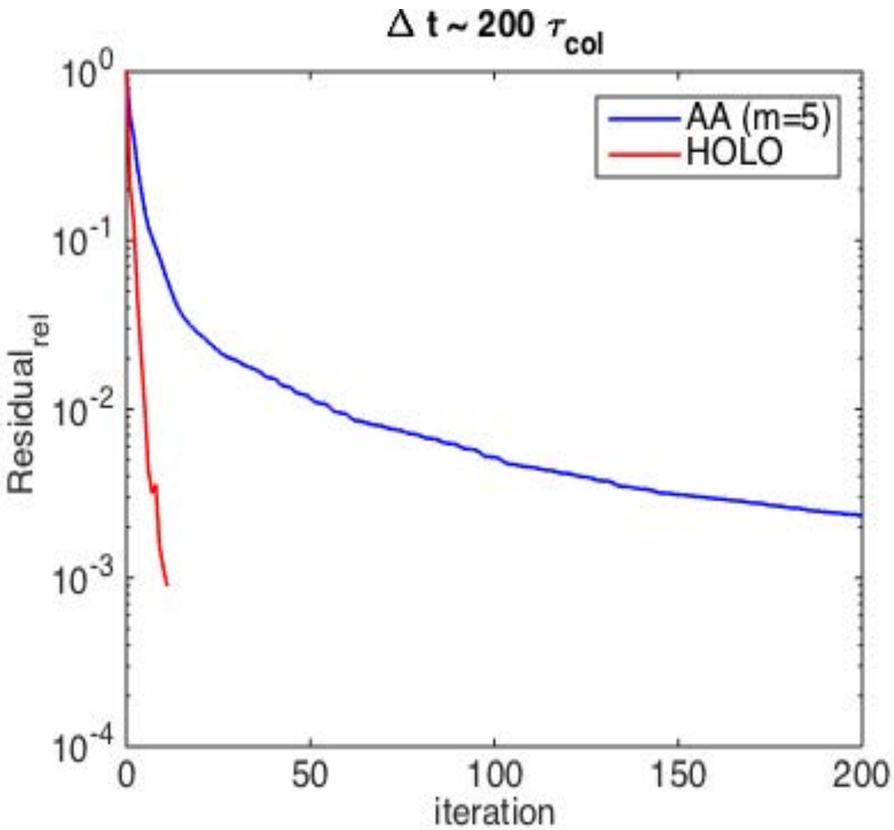

➤ **HOLO is simply a convergence accelerator (i.e., no additional approximations)**

➤ **A significant acceleration in convergence of nonlinear solver is achieved, without changing the solution!**

1D-2V Vlasov-Fokker-Planck equation: Verification and demonstration of long-term accuracy

Verification test: Relaxation of sinusoidal profile

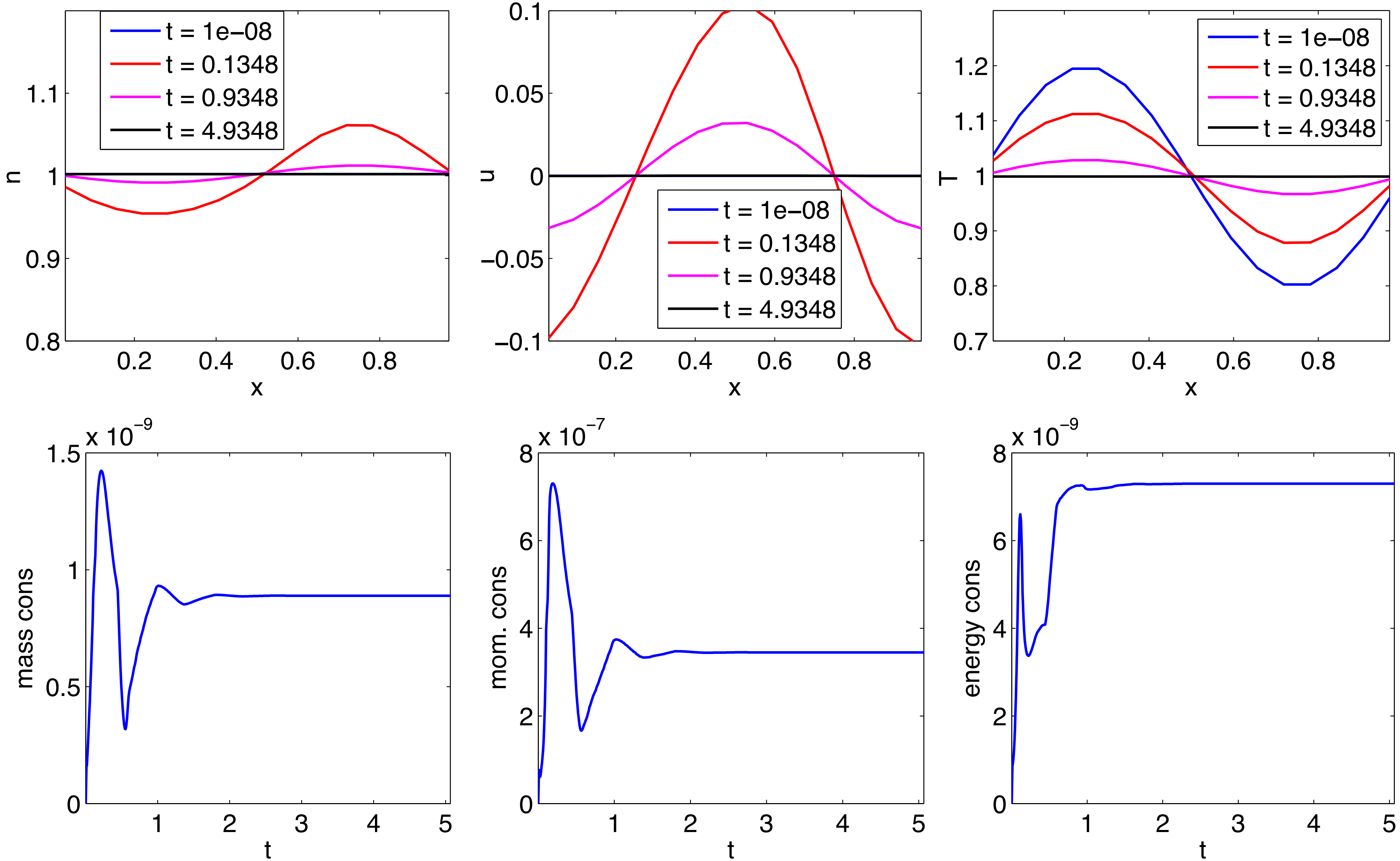

Verification test: Sharp profile relaxation problem

Non-conservative

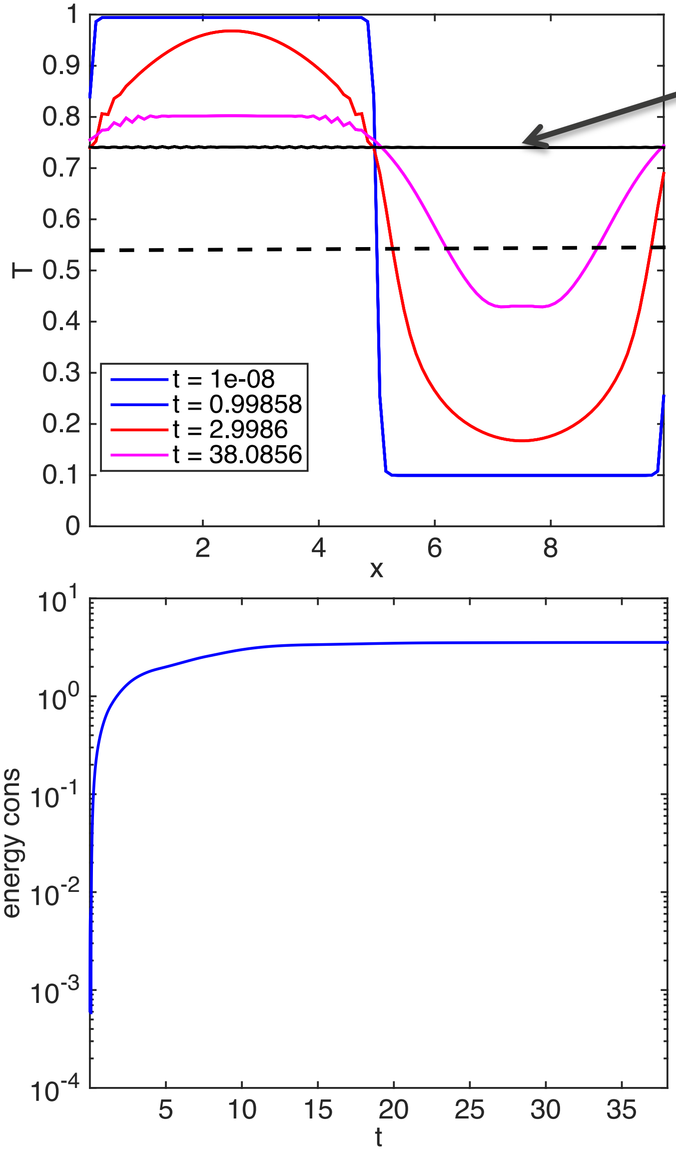

Wrong equilibrium due to numerical heating

Analytical equilibrium

Correct equilibrium achieved

Conservative

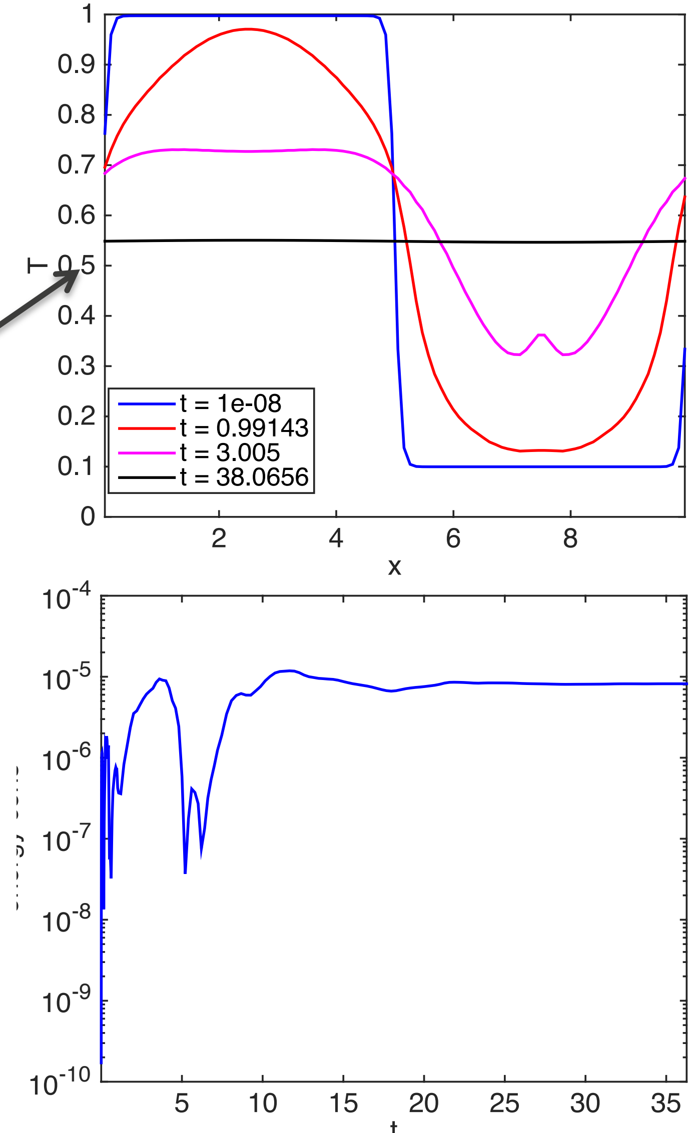

Verification: M=5 Shock (kinetic regime)

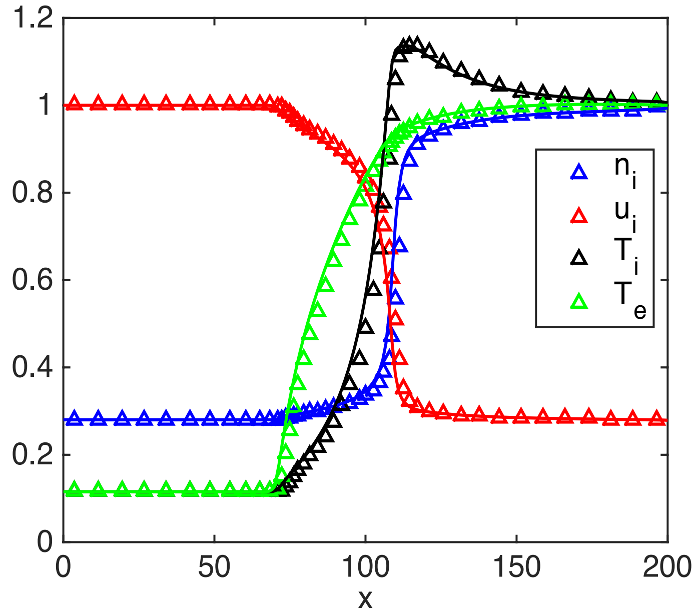

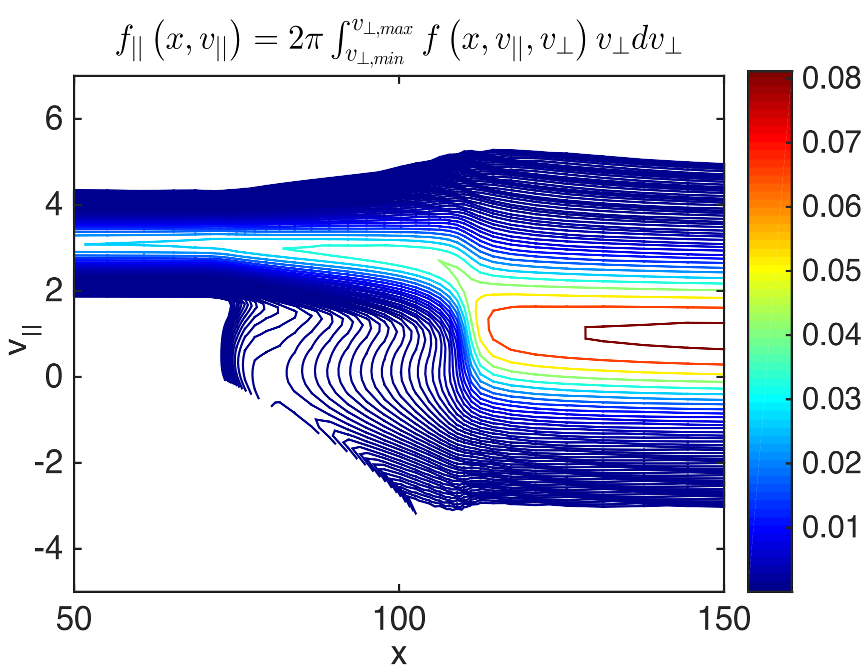

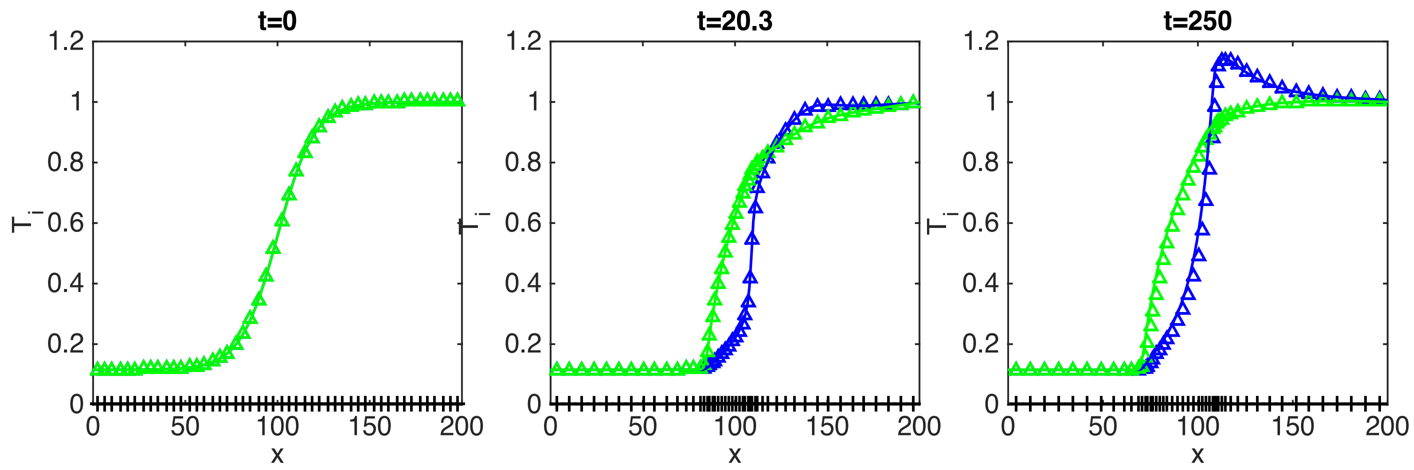

Verification: M=5 Shock conservation properties

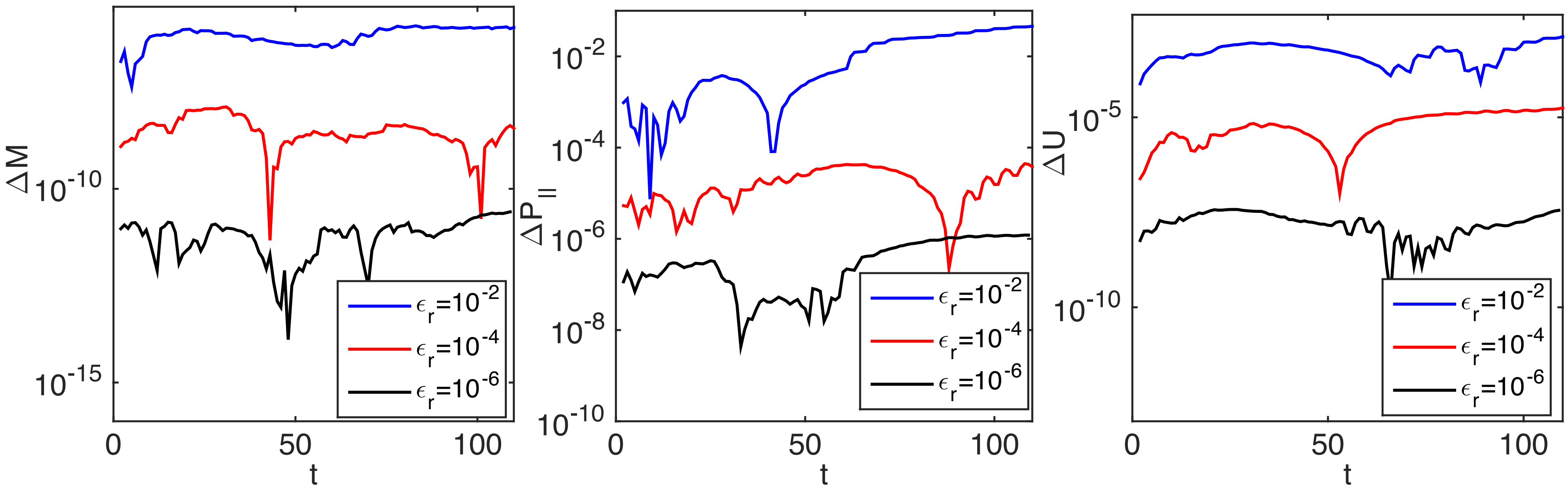

Verification: M=1.5 Shock (fluid regime; HARD)

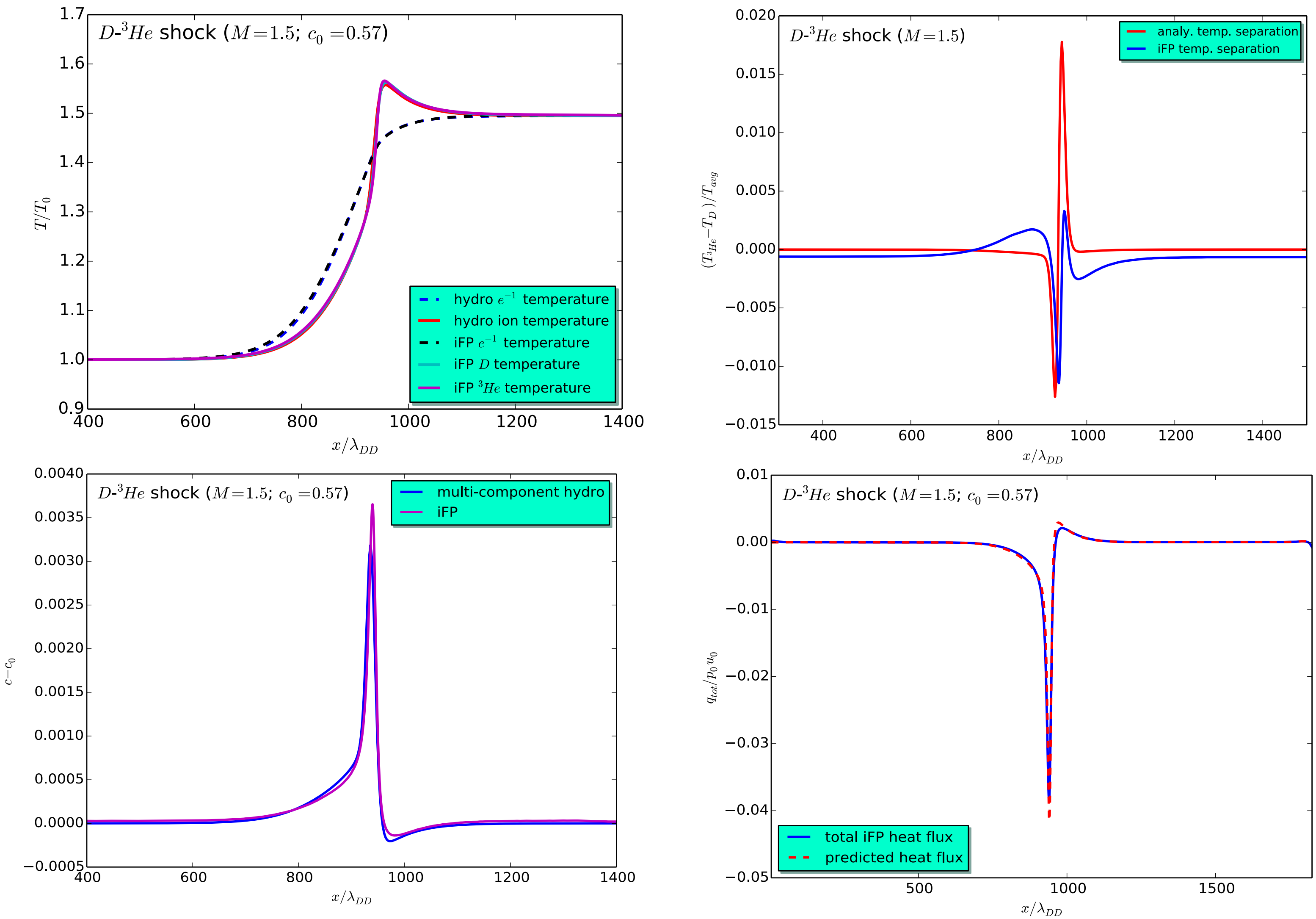

Application: Exploding pusher ICF capsule implosion

The fuel remains fully kinetic throughout the simulation

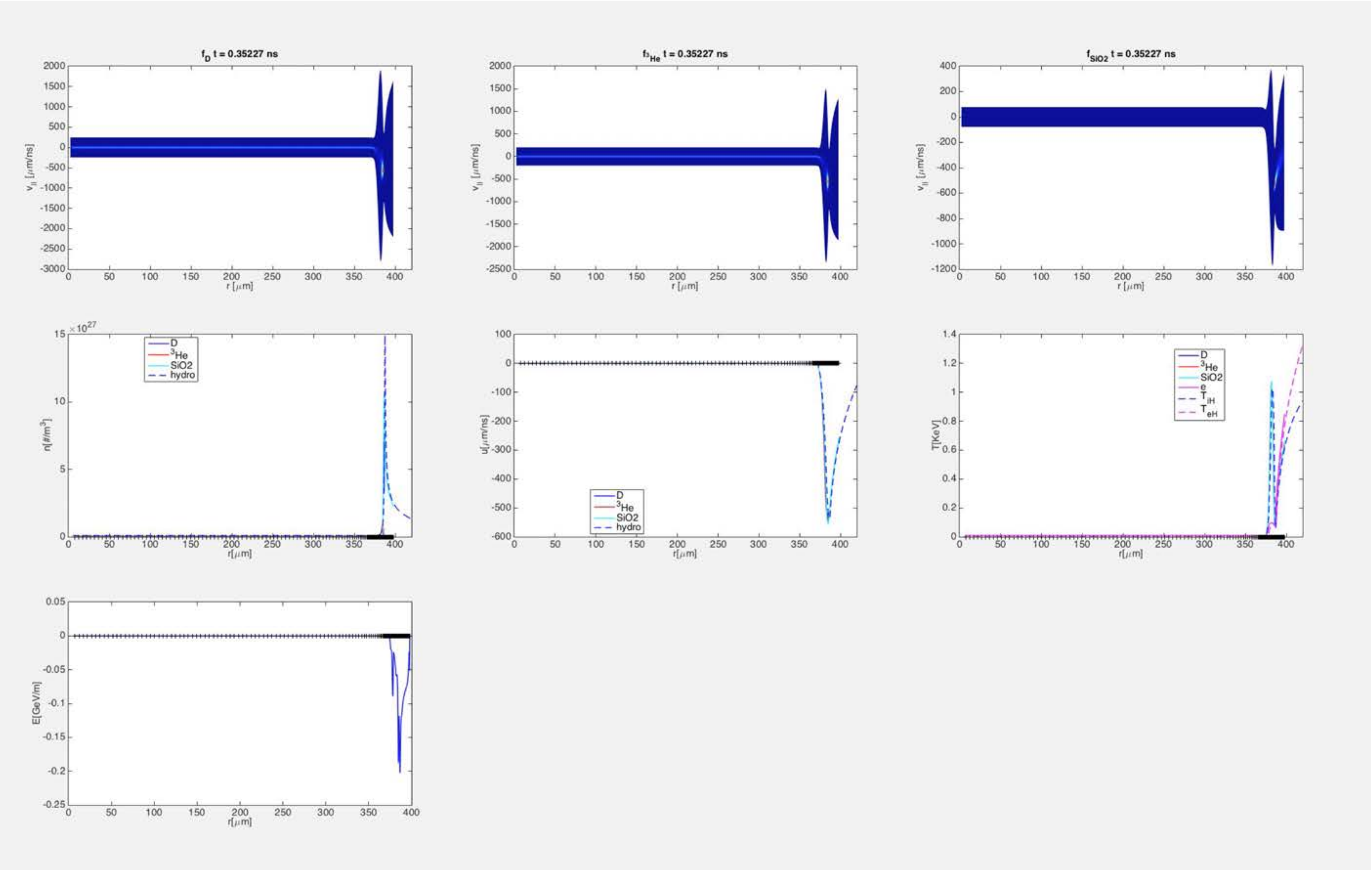

Algorithmic savings in computational complexity

$$\frac{N_{v,static}N_{x,static}}{N_{v,adapt}N_{x,adapt}} = \left(\underbrace{\sqrt{\frac{v_{th,max}}{v_{th,min}}}}_{\sim 300} \times \underbrace{\sqrt{\frac{m_{SiO2}}{m_D}}}_{\sim 3}\right)^2 \times \underbrace{\frac{\Delta x_{max}}{\Delta x_{min}}}_{\sim 100} \sim 10^7$$

$$\frac{\langle \Delta t \rangle_{HOLO}}{100 \times \Delta t_{exp}} \sim 10^5,$$

Simulation takes <24 hours on 400 cores

Conclusions

- **We have derived manifold-preserving algorithms for kinetic plasma simulation**
  - Collisionless (Lagrangian, particle-in-cell)
  - Collisional (Eulerian)
- **Collisionless (PIC): we have solved the 40-year-old algorithmic challenge of developing accurate implicit PIC algorithms**
- **Collisional (VFP): we have demonstrated a truly multiscale algorithm that has enabled routine simulation of ICF spherical capsule implosions with a few hundred cores for a couple of days.**
- **In both cases:**
  - Strict conservation properties have been shown to be critical for long-term accuracy.
  - Significant algorithmic acceleration has been achieved by using nested asymptotic models.
- **We have seen similar benefits in other applications:**
  - Rarefied gas dynamics
  - Radiation transport
  - Ocean modeling